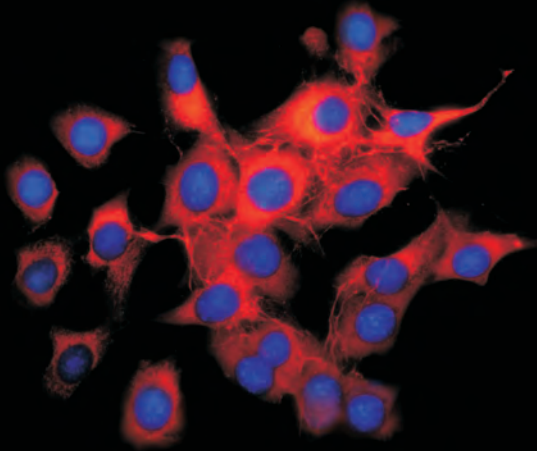


**The WNT/ β -catenin pathway -
Profibrotic signaling in fibroblasts in
Idiopathic Pulmonary Fibrosis**

MONIKA KRAMER



INAUGURALDISSERTATION zur Erlangung des Grades eines **Doktors der Medizin**
des Fachbereichs Medizin der Justus-Liebig-Universität Gießen



édition scientifique
VVB LAUFERSWEILER VERLAG

Das Werk ist in allen seinen Teilen urheberrechtlich geschützt.

Jede Verwertung ist ohne schriftliche Zustimmung des Autors oder des Verlages unzulässig. Das gilt insbesondere für Vervielfältigungen, Übersetzungen, Mikroverfilmungen und die Einspeicherung in und Verarbeitung durch elektronische Systeme.

1. Auflage 2010

All rights reserved. No part of this publication may be reproduced, stored in a retrieval system, or transmitted, in any form or by any means, electronic, mechanical, photocopying, recording, or otherwise, without the prior written permission of the Author or the Publishers.

1st Edition 2010

© 2010 by VVB LAUFERSWEILER VERLAG, Giessen
Printed in Germany



édition scientifique
VVB LAUFERSWEILER VERLAG

STAUFENBERGRING 15, D-35396 GIESSEN
Tel: 0641-5599888 Fax: 0641-5599890
email: redaktion@doktorverlag.de

www.doktorverlag.de

**The WNT/ β -catenin pathway –
Profibrotic signaling in fibroblasts
in Idiopathic Pulmonary Fibrosis**

INAUGURAL-DISSERTATION

zur Erlangung des Grades eines
Doktors der Medizin
des Fachbereichs Medizin der
Justus-Liebig-Universität Gießen

vorgelegt von

Monika Kramer

aus Balve

Gießen 2009

Aus dem Zentrum für Innere Medizin
Medizinische Klinik II,
Direktor: Prof. Dr. med. W. Seeger
Universitätsklinikum Gießen und Marburg GmbH - Standort Gießen

Gutachter: Prof. Dr. O. Eickelberg

Gutachter: Prof. Dr. K. Preissner

Tag der Disputation: 31.08.2010

Meiner Familie

Teile der vorliegenden Arbeit wurden in folgenden Artikeln publiziert:

Königshoff M., Balsara N., Pfaff E. M., Kramer M., Chrobak I., Seeger W., Eickelberg O. Functional Wnt signaling is increased in idiopathic pulmonary fibrosis. PLOS ONE, e2 142 (2008)

Königshoff M., Kramer M., Balsara N., Wilhelm J., Amarie O. V., Jahn A., Rose F., Fink L., Seeger W., Schaefer L., Gunther A., Eickelberg O. WNT1-inducible signaling protein-1 mediates pulmonary fibrosis in mice and is upregulated humans with idiopathic pulmonary fibrosis. *J ClinInvest* 119, 772-787 (2009)

Vorträge und Poster:

Posterpräsentation, Pneumo-Update, Innsbruck. 2007. Kramer M., Königshoff M., Eickelberg O. WNT-/WISP1 signaling in lung fibroblasts: Novel profibrotic mediators in IPF.

Vortrag, Sektion Zellbiologie der Deutschen Gesellschaft für Pneumologie und Beatmungsmedizin e.V. 2008. Kramer M., Königshoff M., Eickelberg O. WNT-/WISP1-Signaltransduktion in Lungenfibroblasten: Neue profibrotische Mediatoren in der idiopathischen pulmonalen Fibrose.

I Content

I Content	I
II Figures	IV
III Tables	IV
IV Abbreviations	V
V Summary	X
VI Zusammenfassung	XI
1. Introduction	1
1.1 Interstitial lung diseases	1
1.2 Idiopathic pulmonary fibrosis	2
1.2.1 Epidemiology	2
1.2.2 Clinical and histopathological features	2
1.2.3 Pathomechanisms of idiopathic pulmonary fibrosis	5
1.3 WNT signaling	8
1.3.1 WNT family of signaling molecules – classification and physiology	8
1.3.2 The WNT/ β -catenin signaling pathway	8
1.3.2.1 WNT/ β -catenin signaling in diseases	10
1.3.2.2 WNT/ β -catenin signaling in the lung and in IPF	11
1.3.3 WNT1-inducible signaling protein 1 in IPF	12
2. Hypothesis and aim of the study	14
3. Materials and Methods	16
3.1 Materials	16
3.1.1 Cells / Cell line	16
3.1.2 Machines / Software	16
3.1.3 Reagents	16
3.1.3.1 Chemicals and biochemicals	16
3.1.3.2 Ligands, recombinant proteins	17
3.1.3.3 qRT-PCR reagents	18
3.1.3.4 Antibodies	18
3.1.3.5 Buffer	18
3.1.3.6 Gels	20
3.1.4 Kits	21
3.2 Methods	21

3.2.1 Cell culture	21
3.2.2 [³ H]-thymidine proliferation assay	21
3.2.3 Protein extraction and quantification	22
3.2.4 SDS polyacrylamide gel electrophoresis.....	22
3.2.5 Immunoblotting	23
3.2.6. Densitometry	23
3.2.7 Sircol Collagen Assay	24
3.2.8 RNA isolation and measurement.....	24
3.2.9 cDNA synthesis.....	25
3.2.10 Quantitative reverse transcription polymerase chain reaction (qRT-PCR).....	25
3.2.10.1 Measurement of fluorescence with SYBR Green I.....	26
3.2.10.2 Primerdesign and efficiency test	27
3.2.10.3 Melting curve analysis	28
3.2.10.4 Quantification and analysis of data	28
3.2.11 DNA agarose gelelectrophoresis.....	29
3.2.12 Immunofluorescence	29
3.2.13 Statistical analysis	30
4. Results	31
4.1 Analysis of occurrence of WNT/ β -catenin signaling in fibroblasts.....	31
4.1.1 Phenotype of NIH-3T3 fibroblasts.....	31
4.1.2 Expression analysis of WNT pathway components in fibroblasts.....	32
4.1.3 Induction of WNT/ β -catenin signaling in fibroblasts by stimulation with WNT3a	35
4.2 Functional analysis of paracrine effects of WNT3a on fibroblasts.....	37
4.2.1 Effects of WNT3a on lung fibroblast proliferation.....	37
4.2.2 Effects of WNT3a on collagen deposition of lung fibroblasts.....	38
4.2.3 Effects of WNT3a on gene expression of ECM molecules and (myo-) fibroblast markers	40
4.3 Functional Analysis of effects of WISP1 on fibroblasts	42
4.3.1 Effects of WISP1 on fibroblast proliferation	42
4.3.2 Effects of WISP1 on collagen deposition of fibroblasts	43
4.3.3 Effects of WISP1 on gene expression of ECM molecules and (myo-) fibroblast markers	45
5. Discussion	47
5.1. Fibroblasts in IPF pathogenesis.....	47

5.2. WNT/ β -catenin signaling in lung fibroblasts	48
5.3. Conclusions and future perspectives in regard to IPF pathogenesis	54
6. Appendix	56
6.1 Primer sequences and amplicon sizes	56
6.2 Dissociation curves.....	59
7. References	62
8. Erklärung.....	69
9. Danksagungen	70

II Figures

Figure 1. Scheme of DPLD classification ¹	1
Figure 2. Survival of IPF/UIP patients compared to NSIP and other DPLD.....	2
Figure 3. Histopathological changes in IPF.	5
Figure 4. Hypothetical scheme of the primary pathogenic events in IPF ¹²	7
Figure 5. Overview of canonical WNT signaling pathway ³⁶	9
Figure 6. Immunohistochemical stainings of β -catenin in ATII cells and fibroblasts in IPF lungs.	12
Figure 7. Scheme of CCN family members and their functional domains ⁶⁷	13
Figure 8. Hypothetical scheme to depict aberrant expression of WNT3a and WISP1 by ATII cells, paracrine binding to lung fibroblasts and possible functional effects.....	15
Figure 9. Phases of a PCR reaction	26
Figure 10. Melting curves	28
Figure 11. Localization and presence of COLT1 and α SMA in the fibroblast cell line NIH-3T3	31
Figure 12. mRNA expression of WNT pathway components in lung fibroblasts	34
Figure 13. WNT responsiveness of fibroblasts.	36
Figure 14. Proliferation of lung fibroblasts after stimulation with WNT3a.....	37
Figure 15. Localization and content of collagen in fibroblasts after stimulation with WNT3a.....	40
Figure 16. mRNA level of ECM molecules and (myo-) fibroblast markers after stimulation with WNT3a.....	41
Figure 17. Proliferation of lung fibroblasts after stimulation with WISP1	42
Figure 18. Localization and content of collagen in lung fibroblasts after stimulation with WISP1	45
Figure 19. mRNA level of ECM molecules and fibroblast markers after stimulation with WISP1	46
Figure 20. Dissociation curves	61

III Tables

Table 1. ATS/ERS Criteria for diagnosis of IPF in absence of surgical lung biopsy ¹	3
Table 2. Histologic features of Usual interstitial pneumonia (UIP) ¹	4
Table 3. Primer sequences and amplicon sizes.	59

IV Abbreviations

m	mili (10^{-3})
μ	micro (10^{-6})
n	nano (10^{-9})

A

A	adenine
AA	amino acid
AIP	acute interstitial pneumonia
ARG	arginase
APC	adenomatous polyposis coli
APS	ammonium persulfate
ATII	alveolar epithelial cell type II
AUC	area under the curve

B

bp	basepare
BSA	bovine serum albumin

C

$^{\circ}\text{C}$	degree Celsius
C	cytosine
cDNA	complementary deoxyribonucleic acid
CFA	cryptogenic fibrosing alveolitis
CK	casein kinase
Colla1	type I collagen alpha 1
COLT1	collagen type 1
COP	cryptogenic organising pneumonia
Ct	threshold cycle
CTGF	connective tissue growth factor
Cyc	cyclin
Cyr	cystein rich

D

DAPI	4',6-diamidino-2-phenylindole
dd	double distilled
DIP	desquamantative interstitial pneumonia
DNA	deoxyribonucleic acid
dNTP	deoxynucleoside triphosphate
D-MEM	Dulbecco's Modified Eagle Medium
DPLD	diffuse parenchymal lung disease
ds	double stranded
DSH	Dishevelled
DTT	dithiothreitol

E

ECM	extracellular matrix
EDTA	ethylenedinitrilo-N,N,N',N',-tetra-acetate
EGTA	ethylene glycol-bis (2-amino-ethylether)-N,N,N',N',-tetraacetic-acid
EMT	epithelial-to-mesenchymal transition
EtBr	ethidium bromide

F

FAP	familial adenomatous polyposis
FEVR	familial exudative vitreopathy
FITC	fluorescein-5-isothiocyanate
FCS	fetal calf serum
FZD	Frizzled

G

g	gram
G	guanine
Gly	glycin
GSK	glycogen synthase kinase

H

h	hour
---	------

HRP horse radish peroxidase

HX histiocytosis x

I

IB immunoblotting

i.e. id est

ICCH immunocytochemistry

ILD interstitial lung disease

IIP idiopathic interstitial pneumonia

IPF idiopathic pulmonary fibrosis

J

JNK c-Jun N-terminal kinase

K

kDA kilo Dalton

L

LAM lymphangioliomyomatosis

Lef lymphoid enhancer-binding factor

LIP lymphocytic interstitial pneumonia

LRP lipoprotein receptor-related protein

M

m mean

min minutes

MMP matrix metalloproteinase

mRNA messenger RNA

MuLV murine leukemia virus

N

NCBI National Center for Biotechnology Information

n.e. not expressed

NOV nephroblastoma overexpressed

NSIP nonspecific interstitial pneumonia

O

OD_{x nm} optical density at a wavelength of x nanometers

P

Pbgd porphobilinogen deaminase

PBS phosphate-buffered saline

PBST phosphate-buffered saline + 0.1 % Tween 20

PCP planar cell polarity

PCR polymerase chain reaction

Q

q quantitative

qRT-PCR quantitative reverse transcription PCR

R

RB-ILD respiratory bronchiolitis-associated interstitial lung disease

rel relative

RNA ribonucleic acid

rpm rounds per minute

RT room temperature or reverse Transcriptase/Transcription

RT-PCR reverse transcription PCR

S

SDS sodium dodecyl sulfate

SDS-PAGE SDS polyacrylamide gel electrophoresis

s.e.m standard error of the mean

Sfrp Secreted frizzled-related protein

SMA Smooth muscle actin

ss single stranded

T

T thymine

TAE	Tris-acetate-EDTA
TCF	T-cell-specific transcription factor
TE	Tris/ EDTA
TEMED	N,N,N,N'-tetramethyl-ethane-1,2-diamine
TGF	transforming growth factor
TIMP	tissue inhibitor of metalloproteinases
T _m	melting temperature
TRIS	Tris(hydroxymethyl)-aminomethan

W

WISP	WNT1-inducible signaling protein
------	----------------------------------

Further, not listed abbreviations are taken from the valid IUPAC-Nomenclature.

Human genes are printed in italics, their transcripts in capital letters.

Literature references are numbered with superscript Arabic numerals, internet references with superscript Roman numerals.

V Summary

Idiopathic pulmonary fibrosis (IPF) is the most common and most severe form of the idiopathic interstitial pneumonias (IIP). Unresponsive to any currently available therapy it leads to architectural distortion of the lung parenchyma and rapidly to respiratory failure. Although the pathogenesis of the disease is not completely understood, it is well accepted that initial alveolar epithelial cell injury is followed by enhanced fibroblast proliferation and activation to myofibroblasts. These fibroblasts are considered as key effector cells in IPF. The so called fibroblast foci represent hallmark lesions of the disease as they are responsible for the increased ECM deposition that leads to impaired gas exchange and ultimately to fibrosis.

The present study aimed to reveal possible profibrotic paracrine effects of recently identified profibrotic mediators that trigger the disturbed crosstalk between alveolar epithelial cells type II (ATII) and fibroblasts. Recently, WNT/ β -catenin signaling has been demonstrated to be involved in the pathogenesis of IPF. In particular it has been reported that WNT3a and WNT1-inducible signaling protein (WISP) 1 are secreted by ATII cells in IPF.

In the present project it was hypothesized that WNT3a and WISP1 act in a paracrine fashion on fibroblasts, thereby contributing to the impaired ATII cell– fibroblast crosstalk in the pathogenesis of IPF.

It was shown that active WNT/ β -catenin signaling takes place in NIH-3T3 fibroblasts *in vitro* as assessed by Western Blot analysis and quantitative RT-PCR. To reveal functional effects of active WNT/ β -catenin signaling, thymidine [H^3] incorporation proliferation assay, immunofluorescence, Sircol Collagen Assay, as well as quantitative (q) RT-PCR were performed.

WNT3a stimulation of fibroblasts caused a significantly increased production of the extracellular matrix component collagen and led to transcriptional upregulation of fibroblast activation markers. Interestingly, WNT3a stimulation did not affect fibroblast proliferation.

The paracrine effects of WISP-1, which is encoded by a WNT target gene, were analyzed in a comparable way. Like WNT3a, WISP-1 led to enhanced collagen deposition as well as upregulation of fibroblast activation markers. Proliferation of the fibroblasts remained unaffected.

These results provided evidence that both molecules, WNT3a and WISP1, are capable of activating lung fibroblasts and causing increased collagen production in these cells. Therefore it is strongly suggested that WNT3a and WISP-1, which are aberrantly secreted by ATII cells in IPF, are profibrotic mediators that act in a paracrine fashion on fibroblasts during the pathogenesis of this fatal disease.

VI Zusammenfassung

Die idiopathische pulmonale Fibrose (IPF) ist die häufigste und schwerwiegendste Form der idiopathischen interstitiellen Pneumonien (IIP). Sie ist therapierefraktär, führt zu Zerstörung der Architektur des Lungenparenchyms und rasch zu respiratorischem Versagen.

Die Pathogenese der Erkrankung ist größtenteils ungeklärt, wobei neue Studien eine initiale Schädigung von Alveolarepithelzellen (AT) vermuten lassen, woraufhin es zu gesteigerter Fibroblastenproliferation und Aktivierung von Fibroblasten in so genannten Fibroblasten Foci kommt. Diese Foci sind für die gesteigerte Produktion extrazellulärer Matrix verantwortlich, welche zum fibrotischen Umbau des Gewebes führt.

Das Ziel der vorliegenden Studie war es, mögliche Effekte bereits identifizierter profibrotischer Mediatoren zu untersuchen, die die Kommunikation zwischen AT II Zellen und Fibroblasten stören.

Kürzlich konnte gezeigt werden, dass der WNT/ β -catenin Signalweg in der Pathogenese der IPF eine Rolle spielt. Insbesondere wurde gezeigt, dass WNT3a sowie das WNT1-inducible signaling protein-1 (WISP-1) im Rahmen der IPF von ATII Zellen sezerniert werden.

Für das hier vorgestellte Projekt wurde die Hypothese aufgestellt, dass WNT3a und WISP1 parakrin auf Fibroblasten wirken und somit zur gestörten Kommunikation zwischen ATII-Zellen und Fibroblasten im Rahmen der Pathogenese von IPF beitragen.

Mittels Western Blot Analyse und quantitativer RT-PCR konnte gezeigt werden, dass der WNT/ β -catenin Signalweg in NIH-3T3 Fibroblasten *in vitro* aktiviert werden kann. Weitere Effekte einer Aktivierung des WNT/ β -catenin Signalwegs wurden mittels Thymidin [H^3] Proliferations Assay, Immunfluoreszenz, Sircol Collagen Assay und quantitativer RT-PCR durchgeführt.

WNT3a führte zu einer deutlich erhöhten Kollagenproduktion. Zudem kam es zu einer erhöhten Transkription von typischen Markern einer Fibroblastenaktivierung. Interessanterweise beeinflusste WNT3a die Fibroblastenproliferation nicht. Die parakrinen Effekte von WISP-1, welches von einem WNT Targetgen kodiert wird, wurden ebenfalls untersucht. Vergleichbar mit WNT3a führte WISP-1 zu einer erhöhten Kollagenbildung und Fibroblastenaktivierung. Die Proliferationsrate der Fibroblasten änderte sich hingegen nicht.

Die vorliegenden Ergebnisse zeigen, dass beide Proteine, WNT3a und WISP-1, zu einer Aktivierung sowie einer erhöhten Kollagenproduktion von Lungenfibroblasten führen können. WNT3a und WISP-1, welche in IPF verstärkt von ATII Zellen sezerniert werden, wirken parakrin auf Fibroblasten und stellen somit bedeutende profibrotische Mediatoren in der Pathogenese der IPF dar.

1. Introduction

1.1 Interstitial lung diseases

Interstitial lung diseases (ILDs) or diffuse parenchymal lung diseases (DPLDs) are a heterogeneous group of chronic disorders that mainly affect the interstitium of the lung containing the space between the basement membranes of the alveolar epithelium and the capillary endothelium¹. Common feature of these diseases is an increase of connective tissue that ultimately leads to fibrosis accompanied by reduced lung compliance and impaired gas exchange. Without an appropriate therapy this process results in cor pulmonale and respiratory failure². The ILDs are divided into two groups: 1) disorders that occur secondary to a known cause, and 2) disorders that lack an obvious origin. Known causes for ILD are infections, inhalation of anorganic and organic dusts, and circulation disorders. They occur also in association to systemical diseases, like sarcoidosis or collagen vascular diseases. The second group includes all cases with an idiopathic entity, such as the rare pulmonary histiocytosis x (HX), lymphangioleiomyomatosis (LAM), eosinophilic pneumonia and the more frequent idiopathic interstitial pneumonias (IIPs)^{1,3}.

The IIPs include seven entities that can be mainly distinguished by histologic and radiologic patterns as well as clinical features: idiopathic pulmonary fibrosis (IPF), nonspecific interstitial pneumonia (NSIP), cryptogenic organizing pneumonia (COP), acute interstitial pneumonia (AIP), respiratory bronchiolitis-associated interstitial lung disease (RB-ILD), desquamantative interstitial pneumonia (DIP), and lymphocytic interstitial pneumonia (LIP)¹

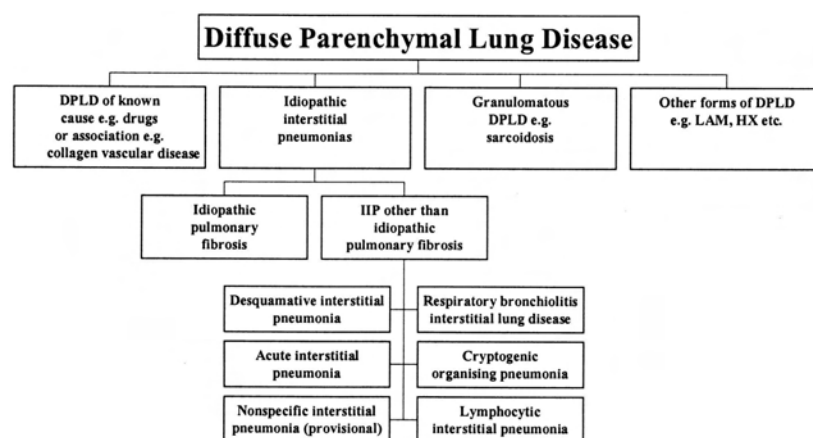


Figure 1. Scheme of DPLD classification¹

1.2 Idiopathic pulmonary fibrosis

1.2.1 Epidemiology

Idiopathic pulmonary fibrosis (IPF), also known as cryptogenic fibrosing alveolitis (CFA), represents the most common form of the IIPs⁴. It mostly occurs in 50 - 70 year old patients with an incidence of 7 – 10 cases per 100.000 and is more common in men^{5,6}. Unresponsive to any currently available therapy, with a median survival time of 2.5 – 3.5 years, it is also considered as the most aggressive form with the worst prognosis of the seven entities^{1,7-9}. The following figure shows the worse survival in IPF patients compared to NSIP and other ILDs¹⁰.

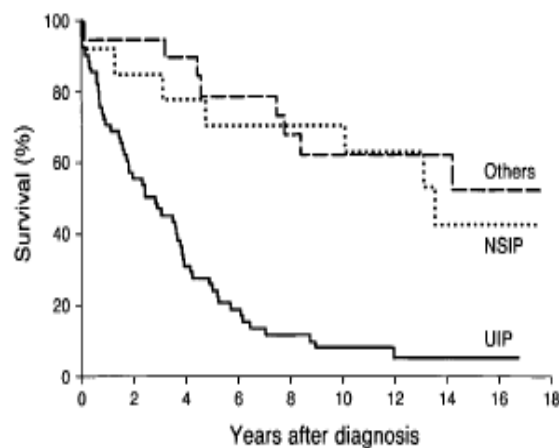


Figure 2. Survival of IPF/UIP patients compared to NSIP and other DPLD

In comparison to NSIP and other DPLDs IPF exhibits the worst prognosis with a median survival about 3 years¹⁰.

1.2.2 Clinical and histopathological features

The patient usually shows dyspnoea and non productive cough. On auscultation often Velcro-type inspiratory crackles are audible over the basal areas of the lung. Digital clubbing can be observed frequently^{1,6,7}. Radiological characteristics are reticular opacities and honeycombing that mainly affect the peripheral, basal and subpleural parts of the lung^{1,4}. Lung function test mostly depicts a restrictive pattern with reduced lung compliance and impaired gas exchange that in the course of the disease leads to decrease of the physical capacity and loss of life quality. In the late stages the patient develops a cor pulmonale. Respiratory failure is the most common reason for lethal outcome of the disorder^{1,2,11}. Because of its devastating character and its lack of effective medicamentous therapy, it is important to differentiate between IPF and the other IIPs^{1,12}. Table 1 shows diagnostic

criteria for IPF, determined by the ATS consensus of 2002, which have to be considered when no surgical lung biopsy is available¹. A correct clinical diagnosis of IPF is probable in presence of all major as well as at least three of the four minor diagnostic criteria in the immunocompetent adult¹.

Major Criteria

- Exclusion of other known causes of ILD such as certain drug toxicities, environmental exposures, and connective tissue diseases
- Abnormal pulmonary function studies that include evidence of restriction (reduced VC, often with an increased FEV1/FVC ratio) and impaired gas exchange [increased P(A-a)O₂, decreased PaO₂ with rest or exercise or decreased DLCO]
- Bibasilar reticular abnormalities with minimal ground glass opacities on HRCT scans
- Transbronchial lung biopsy or BAL showing no features to support an alternative diagnosis

Minor Criteria

- Age > 50 yr
- Insidious onset of otherwise unexplained dyspnoea on exertion
- Duration of illness > 3 mo
- Bibasilar, inspiratory crackles (dry or “Velcro”-type in quality)

Table 1. ATS/ERS Criteria for diagnosis of IPF in absence of surgical lung biopsy¹.

To confirm the diagnosis IPF histologically, it is important to get a surgical lung biopsy. The corresponding histologic pattern is called usual interstitial pneumonia (UIP) and sometimes used synonymously to the term IPF ¹.

Key Histologic Features
<ul style="list-style-type: none">• Dense fibrosis causing remodeling of lung architecture with frequent “honeycomb” fibrosis• Fibroblastic foci typically scattered at the edges of dense scars• Patchy lung involvement• Frequent subpleural and paraseptal distribution
Pertinent Negative Findings
<ul style="list-style-type: none">• Lack of active lesions of other interstitial diseases (i.e., sarcoidosis or Langerhans’ cell histiocytosis)• Lack of marked interstitial chronic inflammation• Granulomas: inconspicuous or absent• Lack of substantial inorganic dust deposits, i.e., asbestos bodies (except for carbon black pigment)• Lack of marked eosinophilia

Table 2. Histologic features of Usual interstitial pneumonia (UIP) ¹.

Architectural distortion of the lung parenchyma as an obligatory consequence of the disorder is marked by fibrosis that consists of dense interstitial extracellular matrix (ECM) alternating with cystically dilated bronchioli, the so called honeycomb cysts. Another characteristic lesion are aggregates of activated myofibroblasts, also referred to as fibroblast foci ^{4,13,5} The prognostic value of fibroblast foci during IPF pathogenesis is controversially discussed. Some authors did not find an association between an increased number of fibroblast foci and a worse prognosis ¹⁴. However, other studies report an inverse correlation between the number of fibroblast foci and the survival of the patient ^{15,16}. According to these reports, an increasing number of fibroblast foci correlates to an impairment of lung function. Therefore, the number

of fibroblast foci can be considered as an important factor that enables indicating the individual prognosis of the patient^{15,16}.

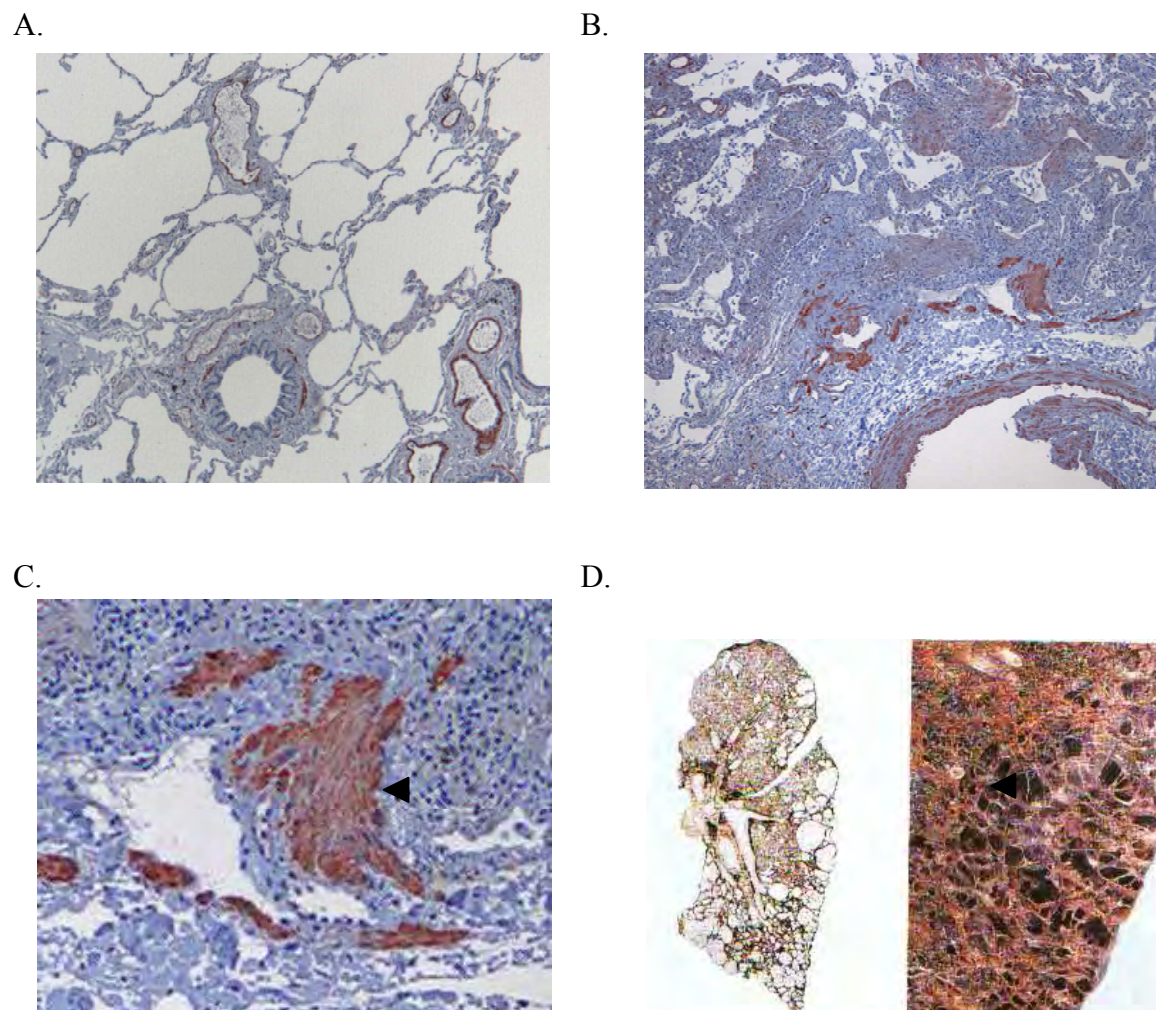


Figure 3. Histopathological changes in IPF.

(A) Structures of a healthy lung (magnification 10×). (B) Structures of an IPF lung (magnification 10×). (C) Fibroblast focus in an IPF lung. The fibroblast focus is indicated with arrow (magnification 40×). Tissue sections were stained for smooth muscle actin, and with hematoxylin and eosin. (D) Honeycomb cystic changes in an IPF lung¹⁷.

1.2.3 Pathomechanisms of idiopathic pulmonary fibrosis

Despite a lot of research efforts, the initial cause and the pathogenic mechanisms of IPF remain enigmatic¹⁸. The (myo-) fibroblast foci and increased interstitial ECM deposition are currently regarded as a consequence of proliferation and activation of fibroblasts, which is initiated by chronic alveolar epithelial cell damage⁴. In the other 6 forms of IIPs the role of inflammation as the preceding trigger for the development of pulmonary fibrosis is more emphasized⁷.

A. Current hypothesis in IPF pathogenesis: epithelial injury as the initial trigger

For a long time most forms of pulmonary fibrosis were regarded as a predominant inflammatory response to an unknown stimulus^{5,18}. In this concept enhanced ECM deposition and fibrosis are caused by inflammatory cells, cytokines, and growth factors in order to repair the affected tissue¹⁹. In IPF, this hypothesis has been challenged. This is mainly due to several observations: 1) anti-inflammatory drugs do not lead to the expected therapeutic success, and 2) IPF patients' histology does not exhibit high, but rather mild to moderate degrees of inflammation at different stages of the disease^{7,12,18}. Thus, the current suggestion of IPF pathogenesis abandons the emphasis of inflammation and claims repetitive epithelial microinjuries and subsequent cell death next to hyperplastic and inappropriate repair processes as key pathogenic mechanisms in the development of the disease. Consequences are disruption of the epithelial integrity in the alveoli lacking the ability to re-epithelialize, and the release of profibrotic cytokines and growth factors by the damaged epithelial cells. Migration and accumulation of fibroblasts occur subsequently and further on generate enhanced ECM deposition^{7,12}. However, the "inflammatory" concept should not be excluded from the pathogenesis, but rather included as an associating factor into the more prominent force: the alveolar epithelial injury^{2,12}.

B. Fibroblasts in IPF pathogenesis: key effector cells

As members of the connective tissue cell family, fibroblasts are mesenchymal derived cells. They occur in every tissue, where they can be activated to synthesize and secrete components of the ECM that consists of collagens, elastins, and proteoglycans. In the lung, fibroblasts play a crucial role for maintaining normal lung function, ventilation, and gas exchange^{20,21}. By providing an organ with ECM as a tissue scaffold during repair processes, fibroblasts are pivotal for tissue remodelling and wound healing processes²². Contributing to that function, they additionally possess the ability to secrete growth factors, cytokines, express integrins or release oxidants, thereby being able to influence other cell types' proliferation, migration, and apoptosis²³. Fibroblasts do not appear in a fixed phenotype. Depending on the circumstances and requirements of their surroundings, they can change their phenotype and appear as a migratory, proliferative phenotype or as profibrotic, activated phenotypes²⁴.

In IPF pathogenesis, fibroblasts can be regarded as key effector cells. They are responsible for the impaired physiological balance of ECM deposition that finally leads to destruction of normal lung architecture and accumulation of fibrotic scar tissue. Fibroblast foci represent

hallmark lesions of the disease. They comprise myofibroblasts that constitute a synthetically active contractile phenotype and secrete an overabundance of ECM components^{13,25,26,27}, which also occurs in skin wound healing processes²². The fact that they are localized in the subepithelial layer in close proximity to injured alveolar epithelium underlines the assumption that an impaired crosstalk between both cell types mediates the progression of the disease^{13,25}. It remains unclear, which mechanism initially triggers the differentiation of the fibroblasts, but a possible role of local growth factors and cytokines is well accepted^{8,28}. Source of these profibrotic molecules are probably hyperplastic alveolar epithelial cells type II (ATII), which release growth factors and cytokines^{7,12} that can influence phenotype and behaviour of fibroblasts in a paracrine fashion. Identification of such possibly profibrotic mediators and analysis of their effects could provide new information about pathogenic mechanisms in IPF, including crosstalks to signaling pathways that are already known to be involved in the progression of the disease. Thereby, new therapeutical options targeting these mediators may be developed.

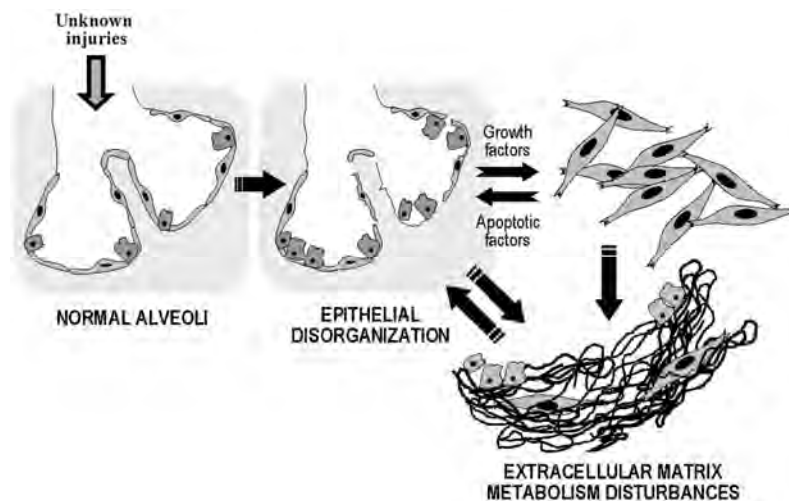


Figure 4. Hypothetical scheme of the primary pathogenic events in IPF¹².

Alveolar epithelial cells are activated by unknown injuries and release factors that influence phenotype and behaviour of fibroblasts. In the lesion, myofibroblasts can induce epithelial cell apoptosis and disruption of basement membrane contributing to abnormal re-epithelialization. Additionally, activated fibroblasts secrete excessive amounts of ECM¹².

1.3 WNT signaling

1.3.1 WNT family of signaling molecules – classification and physiology

The WNT family of signaling molecules consists of secreted glycoproteins that play an important role as ligands in receptor mediated signaling pathways. The name WNT is composed of two homologous genes: Wingless (*Wg*), a segment polarity gene from *Drosophila* and *Int1*, a proto-oncogene associated with mammary tumors^{29,30}.

In mammals, 19 WNT members are known, encoded by *Wnt* genes. Names of gene and corresponding protein are the same: WNT 1, 2, 2b, 3, 3a, 4, 5a, 5b, 6, 7a, 7b, 8a, 8b, 9a, 9b, 10a, 10b, 11 and 16¹. The proteins, in length of usually 350-400 amino acids (aa), have a highly conserved sequence that is characterized by a signal domain and a cysteine pattern^{31,32}. Before they are secreted, WNT ligands undergo posttranslational modifications, such as glycosylation and palmitoylation. In palmitoylated form, the ligands, like the representative WNT3a, transduce signals into the cytoplasm of different target cells^{33,34}. Signal transduction in the cytoplasm of different target cells leads to changed expression of various target genes and subsequently can influence proliferation, migration, differentiation and cell fate specification. Active WNT signal transduction is a key process during development and is also described in cancer^{35,36}. Currently, three different pathways are known, which describe the downstream signaling of WNT binding to the cell surface. The first and best understood pathway is the β -catenin dependent canonical WNT pathway (WNT/ β -catenin pathway). The second involves Ca^{2+} and further one is associated with the c-Jun N-terminal kinase (JNK). The latter one is also related to as the Planar Cell Polarity Pathway (PCP)^{31,35-38}.

1.3.2 The WNT/ β -catenin signaling pathway

WNT/ β -catenin signaling, also referred to as canonical WNT signaling, involves the transcriptional regulator β -catenin as an intracellular key molecule. Known ligands that induce this pathway are: WNT 1, 2, 2b, 3, 3a, 7a, 7b, 8, 10. In absence of WNT, the intracellular β -catenin level is low, because the molecule is destined to proteasome-mediated degradation by a so-called degradation complex. This complex is composed of Axin, adenomatous polyposis coli (APC) and glycogen synthase kinase- (GSK) 3β . GSK 3β together with casein kinase γ (CK γ) is responsible for constitutive phosphorylation of β -catenin that in this form is targeted for ubiquitination and afterwards degradation^{31,35}. When WNT/ β -catenin signaling is activated, this degradation pathway is inhibited. In this case, WNT ligands

bind to the seven transmembrane receptors Frizzled (FZD) that form the primary receptors at the cell membrane³⁹. The following Fzd receptors are already known to interact with WNT and activate the signaling cascade: Fzd 1, 2, 3, 4, 5, 7, 8 and 9¹. WNTs bind to an extracellular cysteine rich domain of one of these receptors that builds a complex with a single pass transmembrane coreceptor. This coreceptor, in *Drosophila* encoded by the gene *arrow*, is called low density lipoprotein receptor-related protein (LRP) 5 or 6⁴⁰. After ligand binding to the receptors the signal is transduced to Dishevelled (DSH), another intracellular pathway component with the ability to interact with Axin. Axin is recruited by DSH and binds directly to the cytoplasmic tail of LRP5/6⁴¹. Without Axin the degradation complex is inhibited and β -catenin is not phosphorylated anymore. Subsequently, hypophosphorylated β -catenin accumulates in the cytoplasm and is translocated to the nucleus. There it replaces the repressing factor Groucho from transcription factors of the T-cell-specific transcription factor/lymphoid enhancer-binding factor (TCF/LEF) family and thereby activates the transcription of WNT target genes^{31,35,42}. Effects of WNT/ β -catenin signaling differ cell-type specific. Hence, the target cell determines the response³⁵.

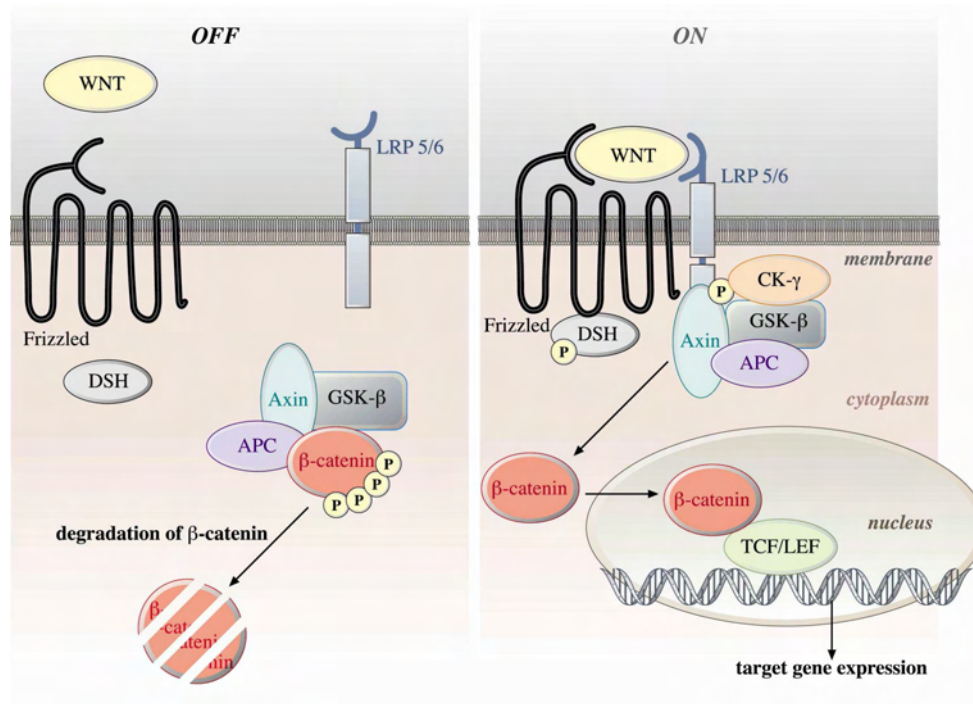


Figure 5. Overview of canonical WNT signaling pathway³⁶.

Degradation of cytosolic β -catenin in absence of WNT(left). Signaling cascade in presence of WNT ligand at the cell surface (right).

According to the fact that different cell types or tissues respond in distinct manners to WNT binding, ligand-receptor affinity varies depending not only on the particular WNT ligand and FZD receptor, but also on the cell type³⁵.

Extensive research, mostly via microarray analysis, has led to the identification of numerous direct and indirect WNT target genes. One group of WNT-inducible genes are components of the pathway themselves, indicating a feedback control^{35,1}. Other target genes, such as the cell cycle regulators *myc*⁴³ and Cyclin D1 (*CycD1*)^{44,45} or the matrix metalloproteinase 7 (*Mmp7*) /matrilysin⁴⁶ are listed on the WNT Homepage. They point the functional relevance of WNT signaling in different organs, tissues and cells. Mutations or other defects causing disturbed or constitutively active signal transduction can result in developmental abnormalities or diseases³⁵.

1.3.2.1 WNT/ β -catenin signaling in diseases

The fundamental importance of WNT signaling during development and for balanced tissue maintenance is reflected in diseases occurring in association to mis-regulated signaling. Most of them were firstly identified by mutant phenotype analysis in mice, but actually numerous human diseases can be correlated to disturbed WNT/ β -catenin signaling.

Currently, the most frequent and therefore best studied issue is the relation of WNT signaling to cancer. As many WNT target genes are involved in proliferation, apoptosis, and cell cycle regulation – functions that are out of order during tumorigenesis – a contribution of the canonical pathway to these processes suggests itself⁴⁷. Mutations in Axin, part of the degradation complex result in increased canonical signaling and were found in colon cancer as well as hepatocellular carcinoma^{48,49}. Constitutive activation of the pathway can also be caused by truncation of APC or mutations in β -catenin and are reported to induce colon cancer and familial adenomatous polyposis (FAP), a hereditary disorder characterized by precancerous polyps⁵⁰. Involvement of WNT signaling in pancreatic, ovarian, prostate and mammary cancer has been also reported⁵⁰. In lung cancer it was shown that overexpression of WNT1 and some of its target genes is associated with tumor progression and impairment of the prognosis^{51,52}. Also, it was already suggested that a WNT inhibitory factor has the capacity to arrest cell growth in lung cancer⁵³.

Wound healing and skin represent other areas, in which the role of canonical signal transduction is examined. Active WNT/ β -catenin signaling is involved in the recruitment of

fibroblasts and influences their behaviour, thereby playing a role in fibromatosis and wound healing in general^{54,55}. Furthermore it contributes to the development of fibrotic diseases that are characterized by pathologic tissue remodelling⁵⁶⁻⁵⁸:

In experimental liver fibrosis the expression of WNT and FZD was demonstrated. Additionally, WNT antagonism was able to inhibit activation of hepatic stellate cells that represents one of the main pathologic events in liver fibrosis⁵⁶. WNT4 and WNT/ β -catenin signaling respectively were reported to be involved in the pathogenesis of renal fibrosis as well as WNT inhibition was able to affect the progression^{57,58}.

In sum, many reports have established involvement of WNT/ β -catenin signaling in cancer and fibrotic diseases. From this emanate possible approaches for new therapies that require further investigation in the field.

1.3.2.2 WNT/ β -catenin signaling in the lung and in IPF

The WNT/ β -catenin signaling pathway plays a fundamental part in lung development. Several WNT proteins are expressed in the lung, in the adult organ as well as during development³⁵. In mice with deficiency of WNT5a or WNT7b various lung defects affecting both epithelium and mesenchymal cells could be observed at different developmental stages. Given that these two proteins are expressed only in the epithelium, the defects can be referred to autocrine and paracrine signaling mechanisms as well⁵⁹. Lack of β -catenin, the intracellular key molecule of canonical signaling, leads to misformation of the distal airways that are required for appropriate gas exchange⁶⁰. These and other observations that reflect the relevance of WNT in lung development indicate that it can also be involved in pathologic processes in the adult organ. This suggestion was followed by Chilosì and colleagues⁶¹, who reported an increase of β -catenin in fibroblast foci and alveolar epithelial cells type II (ATII) indicative of an aberrant activation of WNT signal transduction in IPF⁵⁹. Furthermore, in our laboratory an increase of functional WNT signaling in IPF was observed. More precisely, we found an increase of WNT1, 7b and 10b, Fzd2 and 3, β -catenin, and Lef1 expression in IPF lungs and demonstrated a significant increase of WNT signaling in ATII cells derived from IPF patients. Immunohistochemical stainings revealed that β -catenin localization in ATII cells of IPF lungs is enhanced in the cytoplasm and nucleus, whereas it is more membranous in donor lungs, also indicating an activation of the signaling in IPF.

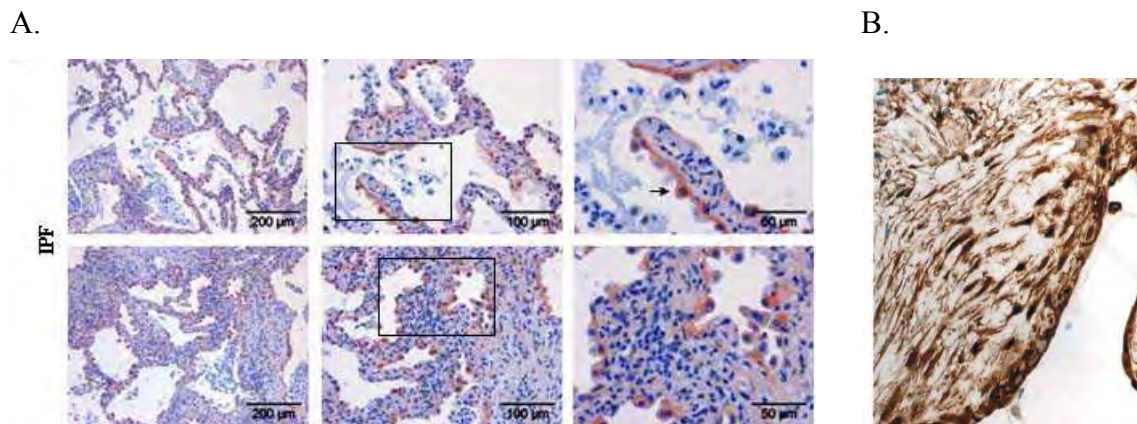


Figure 6. Immunohistochemical stainings of β -catenin in ATII cells and fibroblasts in IPF lungs. (A) Cytoplasmatic and nuclear accumulation of β -catenin in ATII cells (arrow)⁶². (B) Nuclear accumulation of β -catenin in fibroblasts in subepithelial fibroblast foci⁶¹

Furthermore, unbiased microarray screens have revealed an increased expression of WNT target genes, such as matrix metalloproteinase (*Mmp*) 7, or secreted frizzled-related protein (*Sfrp*) 2 in IPF^{63,64}.

To reveal the functional significance of WNT/ β -catenin signaling activation in IPF further investigation is required. Both, characterization of the stimuli that cause the β -catenin elevation and elucidation of the resulting mechanisms could provide new targets for inhibiting the progression of the disease.

1.3.3 WNT1-inducible signaling protein 1 in IPF

WNT1-inducible signaling protein (WISP) 1 is encoded by the WNT target gene *Wisp1* and was first discovered in a monkey epithelial cell line. It belongs to the CCN family of growth factors⁶⁵. This family consists of six regulatory, multimodular cysteine-rich proteins about 30-40 kDa⁶⁶: cysteine-rich 61 (Cyr61/CCN1), connective tissue growth factor (CTGF/CCN2), nephroblastoma overexpressed (NOV/CCN3), WNT1-inducible signaling protein 1 (WISP1/CCN4), - 2 (WISP2/CCN5) and - 3 (WISP3/CCN6).

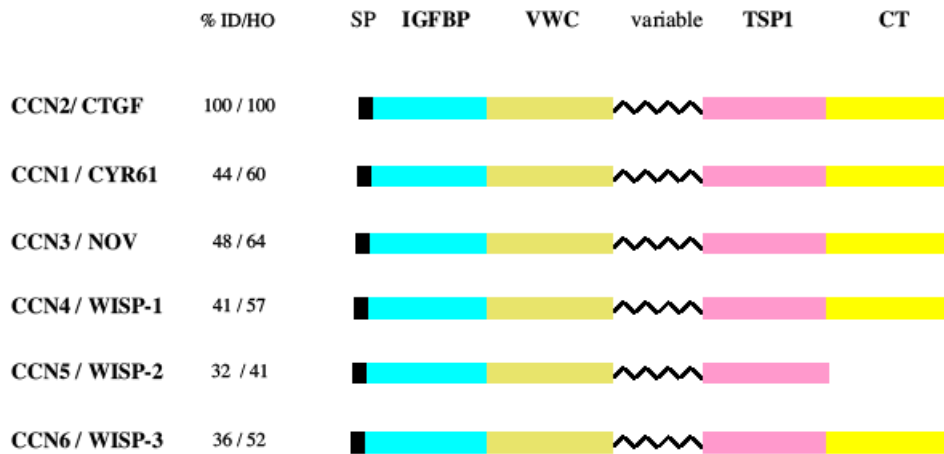


Figure 7. Scheme of CCN family members and their functional domains ⁶⁷.

SP, Signal Peptide ; IGFBP, Insulin-like Growth Factor Binding Protein-like module ; VWC, Von Willebrand Factor-like module ; TSP1, Thrombospondin-like module ; CT, cysteine knot containing family of growth regulator-like module. HO : homology ; ID : identity ⁶⁷.

Their biological function comprises stimulation of mitosis, adhesion, apoptosis, ECM-production, growth-arrest, and migration by transducing signals to target cells like fibroblasts, epithelial cells, endothelial cells, smooth muscle cells, and neuronal cells ⁶⁶. Based on these functions, a role of CCN family members in developmental and pathologic processes is strongly suggested. However, acting mechanisms remain unclear. So far, an integrin-mediated signaling by binding and activating integrins at the cell surface is discussed at least for Cyr61 and CTGF ⁶⁸ that is followed by intracellular signal transduction. *Wisp1* or *Ccn4* was identified as a WNT/ β -catenin downstream target gene that encodes a protein of 367 aa ⁶⁹. Its messenger RNA (mRNA) was found to be upregulated in colon tumors ⁶⁹. This observation accompanied by the ability of WISP1 to have antiapoptotic and proliferative effects on epithelial and mesenchymal cells, strongly indicate a role of WISP1 in tumorigenesis ⁷⁰⁻⁷⁴. For instance, it was already shown to be associated with epithelial cell hyperplasia in breast cancer cell lines ⁷⁵ as well as its presence in lung cancer was described ⁷⁶. In regard to lung, a novel role of WISP1 during IPF pathogenesis was recently revealed ⁷⁷. In our laboratory increased secretion of WISP1 by alveolar epithelial cells type II (ATII) in IPF was observed by an unbiased approach. Furthermore our group found autocrine effects of WISP1 on the ATII cells, which exhibited hyperplasia and expression of profibrotic cytokines after WISP1 treatment. In this context, also paracrine mechanisms of the ligand on fibroblasts seemed probable.

2. Hypothesis and aim of the study

Idiopathic pulmonary fibrosis (IPF) is a devastating disease. It represents the most aggressive form of the idiopathic interstitial pneumonias (IIP). Unresponsive to any currently available therapy it exhibits the worst prognosis of the seven known IIPs^{1,7-9}.

Despite of extensive research, many aspects of the pathomechanisms of IPF remain unclear. Currently, repetitive alveolar epithelial cell type II (ATII) injury and subsequent repair processes are considered as the initial trigger of the disease, which is followed by the activation of fibroblasts^{4,7}. Activated myofibroblasts form fibroblast foci, which represent hallmark lesions of IPF. They secrete abundant extracellular matrix (ECM), what finally leads to the fibrotic transformation of the lung^{4,5,13,25-27}.

New mediators, which can influence the crosstalk between ATII cells and fibroblasts in this context and thereby trigger the progression of IPF were recently identified: WNT/ β -catenin signaling has been demonstrated to be involved in the pathogenesis of IPF⁶¹. In particular, it has been reported that WNT3a and WNT1-inducible signaling protein (WISP) 1 are secreted by ATII cells in IPF^{62,77}. It remains to be analyzed how the crosstalk between ATII cells and fibroblasts is affected by these proteins.

Based on this rationale following was hypothesized for the present project:

The proteins WNT3a and WISP1, which are aberrantly secreted by ATII cells in IPF, act in a paracrine fashion on fibroblasts and thereby contribute to an impaired ATII cell – fibroblast crosstalk in the pathogenesis of IPF.

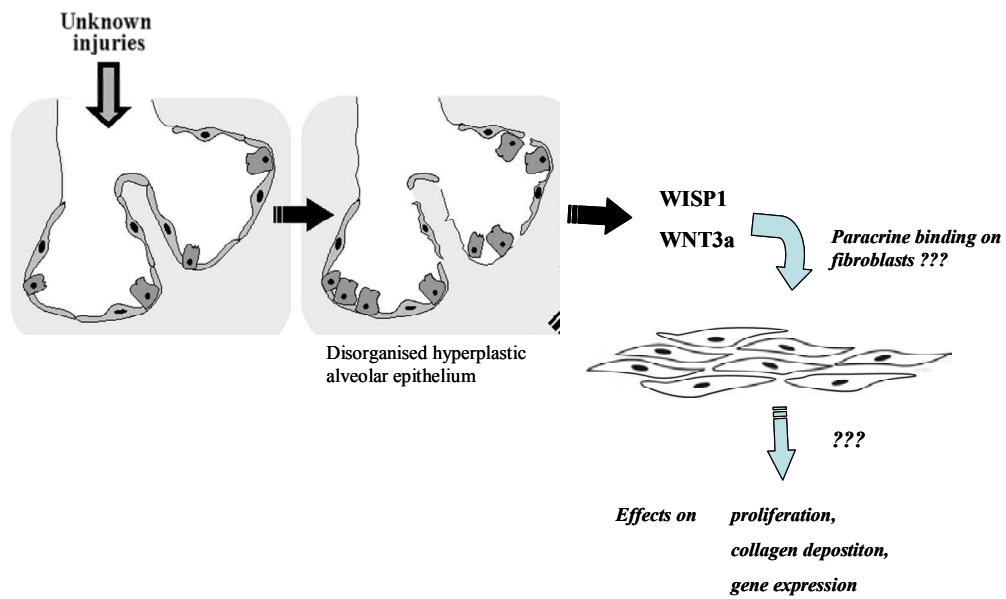


Figure 8. Hypothetical scheme to depict aberrant expression of WNT3a and WISP1 by ATII cells, paracrine binding to lung fibroblasts and possible functional effects.

To test this hypothesis following specific aims were formed:

- Analysis of WNT/ β -catenin pathway expression and activation in fibroblasts.
- Analysis of the effects of WNT3a or WISP1 treatment on
 - a) proliferation ($[^3\text{H}]$ -thymidine proliferation assay)
 - b) collagen production (Sircol Collagen Assay)
 - c) gene expression (qRT-PCR)

3. Materials and Methods

3.1 Materials

3.1.1 Cells / Cell line

NIH-3T3 fibroblasts (Swiss mouse embryo) German Collection of Microorganisms and Cell Cultures (DSMZ), Germany

3.1.2 Machines / Software

Fluorescence microscope; LEICA AS MDW	Leica, Germany
Fusion A153601 Reader	Packard Bioscience, Germany
GS-800TM Calibrated Densitometer	Bio-Rad, USA
Nanodrop ND-100 spectrophotometer	Nanodrop Technologies, USA
PCR-thermocycler	MJ Research, USA
Quantity One software	Bio-Rad, USA
7500 Fast Real-Time PCR System	Applied Biosystems, USA

3.1.3 Reagents

The following chemicals and reagents were purchased from the indicated companies.

3.1.3.1 Chemicals and biochemicals

Acetic acid	Roth, Germany
Acetone	Merck, Germany
Acrylamide solution, Rotiphorese Gel 30	Roth, Germany
Agarose	Promega, USA
APS	Promega, Germany
BSA	Sigma-Aldrich, Germany
β -Mercaptoethanol	Sigma-Aldrich, Germany
Bromphenol Blue	Sigma-Aldrich, Germany

Complete™ Protease Inhibitor	Roche, Germany
Dako Mounting medium	Dako, USA
Dapi	Roche, Germany
DNA Ladder 100bp	Promega, USA
D-MEM	Gibco BRL, Germany
EDTA	Promega, USA
EGTA	Sigma-Aldrich, Germany
Ethanol absolute	Riedel-de Haën, Germany
EtBr	Roth, Germany
FCS	Gibco BRL, Germany
Glycin	Roth, Germany
Glycerol	Merck, Germany
HCl	Sigma-Aldrich, Germany
Igepal CA-630 (NP-40)	Sigma-Aldrich, Germany
Methanol	Fluka, Germany
NaCl	Merck, Germany
Paraformaldehyde	Sigma-Aldrich, Germany
PBS	PAA, Austria
Quick Start™ Bradford Dye Reagent	Bio-Rad, USA
Rotiszint® Eco plus	Roth, Germany
SDS	Promega, USA
Sodium orthovanadate	Sigma-Aldrich, Germany
TEMED	Bio-Rad, USA
TRIS	Roth, Germany
Trypsin/EDTA	Gibco BRL, Germany
Tween-20	Sigma-Aldrich, Germany
[³ H]-thymidine	Amersham Biosciences, Piscataway, New Jersey

3.1.3.2 Ligands, recombinant proteins

WISP1/CCN4 (recombinant, human)	R&D Systems, USA
WNT3a (recombinant, mouse)	R&D Systems, USA
TGF-β1	R&D Systems, USA

3.1.3.3 qRT-PCR reagents

dNTP-Mix	Promega, USA
MgCl ₂ , 50 mM	Invitrogen, Germany
10x PCR buffer (without MgCl ₂)	Applied Biosystems, USA
PCR Nucleotide Mix	Promega, USA
Random Hexamers	Promega, USA
RNase Inhibitor	Applied Biosystems, USA
Reverse Transcriptase MuLV RT	Applied Biosystems, USA

3.1.3.4 Antibodies

<i>primary antibody</i>	<i>origin</i>	<i>dilution</i>	<i>company, catalog number</i>
anti- α SMA	mouse	1:100	Sigma-Aldrich, Germany, A-2547
anti-COLT1	rabbit	1:100	Chemicon, AB765P
anti-Cyclin D1	rabbit	1:3000	Santa Cruz Biotech, USA, sc-753
anti- β -Catenin	rabbit	1:3000	Cell signalling, USA, 9562
anti-Lamin a/c	rabbit	1:3000	Santa Cruz Biotech, USA, sc-20681
<i>secondary antibody</i>	<i>origin</i>	<i>dilution</i>	<i>company, catalog number</i>
Alexa 555 α rabbit IgG	goat	1:1000	Invitrogen, Germany, A21429
FITC α mouse IgG	goat	1:100	Dako, USA, F0479
HRP α rabbit IgG	goat	1:3000	Pierce, USA, 31460

3.1.3.5 Buffer

for Protein extraction:	Lysis-buffer:
	20 mM TRIS pH 7.5
	150 mM NaCl
	1 mM EDTA
	1 mM EGTA
	0.5 % NP-40 (= Igepal CA-630)
	Complete TM Protease Inhibitor [40 μ l/ml]
	Sodium orthovanadate Na ₃ VO ₄

for DNA agarose

gel electrophoresis:

1× TAE buffer:

40 mM Tris-acetate, pH = 8.0

1 mM EDTA, pH = 8.0

for Western Blot analysis

10× SDS-loading buffer:

625 mM Tris-HCl, pH = 6.8

50 % (v/v) glycerol

20 % (w/v) SDS

9 % (v/v) β-mercaptoethanol

0.3 % (w/v) bromophenol blue

SDS-running buffer:

25 mM Tris

50 mM glycine

0.1 % (w/v) SDS

Transfer buffer:

25 mM Tris

192 mM glycine

20 % (v/v) methanol

1× PBST:

1× PBS

0.1 % (v/v) Tween-20

1× TBST:

10 mM TRIS 7.5 pH

150 mM NaCl

Blocking solution:

5 % (w/v) non-fat dry milk

1× PBST

or

5 % (w/v) BSA

1× TBST

Stripping buffer:

62.5 mM Tris-HCl, pH = 6.8

2 % (w/v) SDS

100 mM β -mercaptoethanol**3.1.3.6 Gels****Agarose gel:**

1× TAE buffer

0.2 % Agarose

0.5 $\mu\text{g}/\mu\text{l}$ EtBr**Stacking gel:**

5 % acrylamide: bisacrylamide

125 mM Tris-HCl, pH = 6.8

0.1 % (w/v) SDS

0.1 % (w/v) APS

0.1 % (v/v) TEMED

Resolving gel:

10 % acrylamide: bisacrylamide

375 mM Tris-HCl, pH = 8.8

0.1 % (w/v) SDS

0.1 % (w/v) APS

0.1 % (v/v) TEMED

3.1.4 Kits

	<i>company, catalog number</i>
RNeasy Mini Kit	Qiagen, Germany, 74104
RNase-free Dnase Set	Qiagen, Germany, 79254
Sircol™, Soluble Collagen Assay	Biocolor, UK, S1000
Platinum®SYBR®Green q PCR Super Mix-UDG	Invitrogen, Germany 11733-04

3.2 Methods

3.2.1 Cell culture

NIH-3T3 mouse fibroblasts were cultured in DMEM, supplied with 10 % FCS and maintained in 250 ml culture flasks in an atmosphere of 95-100 % air humidity, 5 % CO₂ at 37 °C. Passaging was carried out in an almost confluent stadium. After one washing step with 1× PBS, 3 ml of Trypsin/EDTA solution were added for 2 minutes (min) to catalyze their detachment from the underlay. This process was stopped by addition of 7 ml culture medium. Afterwards the 10 ml cell suspension either were distributed to new culture flasks in a dilution of 1:10 or seeded accordingly to protocols of upcoming experiments. For stimulation experiments, fibroblasts were kept in medium with reduced serum content of 0.5 % for at least 12 hours (h) to synchronize their metabolic activity before treatment. If not mentioned separately the final concentrations for WISP1 were 1 µg/ml and for WNT3a 100 ng/ml.

3.2.2 [³H]-thymidine proliferation assay

The proliferation assay is based on cleavage-dependent DNA incorporation of thymidine that is marked by the β-radiator ³H. The proliferation rate can be indirectly quantified by measuring the radioactive incorporated thymidine.

Fibroblasts were seeded at a density of approximate 10⁴/well on 48 well plates in 500 µl of culture medium. Adherent fibroblasts were synchronized in 0.5 % FCS medium and stimulated with WISP1 and WNT3a in 200 µl of 0.5 % and 5 % medium, respectively, for 20 h. In the last 6 h of the stimulation, [³H]-thymidine [0.5 µCi/ml] was added to incorporate into the DNA of proliferating cells.

Subsequently, fibroblasts were washed twice with PBS and lysed with 300 µl of sodium

hydroxide (NaOH) per well. 8 ml of Scintillation liquid were added to each sample. Then the measurement of residual radioactivity was performed with a β -scintillation counter, to assess occurrence of proliferation.

3.2.3 Protein extraction and quantification

Fibroblasts were plated on 10 cm diameter culture dishes or six well plates at a density of 60 % or 90 %, respectively, and incubated until they were adherent. Synchronisation in 0.5 % FCS medium was followed by stimulation of the fibroblasts with WISP1, WNT3a or TGF β -1. After the stimulation endpoints, proteins were lysed in lysis buffer (described in 3.1.3.5) and carefully harvested by scraping with a rubber policeman. The suspensions were transferred to Eppendorf tubes and incubated on ice for 30 min. During that time the tubes were vortexed each 10 min. After centrifugation at 13.000 rpm and +4 °C for 15 min, the supernatant containing the proteins was collected.

The protein concentration in the cell extracts was determined colorimetrically using the Bradford Protein Assay. This method is used for measurement of the protein content in solutions. It is based on a change in the absorption spectrum of Coomassie Brilliant Blue G-250 dye when the dye binds to cationic nonpolar and hydrophobic side chains of amino acids. After binding the reagent is stable in its deprotonated anionic sulfatic form. Accompanied by deprotonation it changes to a blue colour. The absorption maximum moves from 465 nm to 595 nm. Accordingly, the absorption changes proportional to the amount of proteins in the sample.

To perform the measurement, protein probes were diluted 1:10. Each sample was mixed with 200 μ l of the Bradford dye and transferred to a 96well plate. Different dilutions of bovine serum albumin (BSA) (0.05; 0.1; 0.2; 0.3; 0.4; 0.5; 0.6 μ g/ μ l) were used as a protein standard to construct a protein standard curve.

After 15 min incubation, the absorption was measured at a wavelength of 570 nm in a Fusion A153601 Reader. The corresponding protein concentrations were calculated by interpolation using the standard curve.

3.2.4 SDS polyacrylamide gel electrophoresis

In order to perform Western Blot analysis, protein extracts were separated by SDS polyacrylamide gel electrophoresis (SDS-Page). The dissociating agent SDS denatures the

proteins, binds to the polypeptides and provides a consistent negative charge to the polypeptides, so that they migrate to the positive electrode. The mobility of the proteins increases linear to the protein size. Smaller molecules migrate faster than larger ones and the proteins can be separated according to their molecular weight. For the separation two polyacrylamide gel layers were used: a resolving gel and a stacking gel, which were produced according to the recipe, described in 3.1.3.6. Ammonium persulfate (APS) and N,N,N,N,N'-tetramethylethylenediamine (TEMED) were added at last to initiate the polymerisation of the gels. 20 µg of each protein sample were mixed with 10× SDS-loading buffer and denaturated in a water bath at 100 °C for 5 min. After loading the proteins onto the gel, electrophoresis was performed in SDS-running buffer at 110 V.

3.2.5 Immunoblotting

After separation of the proteins by SDS-Page, immunoblotting (IB) was performed to visualize and detect specific proteins. The proteins were transferred to 0.25 µm pure nitrocellulose membrane in transfer buffer at 120 V for 1 h. Membranes were blocked in blocking solution at room temperature (RT) for 1 h. For blocking either PBST with 5 % milk or TBST with 5 % BSA were used, depending on manufacturers' recommendations for the corresponding antibody. Afterwards the nitrocellulose membranes were incubated with the appropriate primary antibody, diluted in the blocking solution, at 4 °C overnight. Concentrations of the different antibodies are listed in 3.1.3.4.

The incubation was followed by washing the membranes three times for 10 min with 1×TBST or 1×PBST, respectively, and then incubated with horse radish peroxidase labelled secondary anti-rabbit antibody for 1 h at RT. After washing, the protein detection was performed by chemiluminescence with the help of an enhanced chemiluminescence IB system and exposure to radiographic film. To be able to re-probe the membranes with another antibody, they were stripped with stripping buffer (described in 3.1.3.5) at 52 °C for 5 min, washed, blocked and subsequently treated with antibodies as described above.

3.2.6. Densitometry

To perform densitometric analysis, a GS-800TM Calibrated Densitometer and 1-D analysis software Quantity One were used. Protein expression was normalized to Lamin A/C levels, which served as a loading control.

3.2.7 Sircol Collagen Assay

The Sircol Collagen Assay can be used for measuring collagen content of cells or tissues *in vitro* quantitatively by dye-binding. The dye contains Sirius Red Anions with acid sulphonic side chains that can bind to the basic amino acids of collagen, particularly to the helical [Gly-x-y]_n structure of all collagens. Specific binding to collagen is furthermore enforced by the parallel attachment of the long dye molecules to the likewise long and rigid triple helix structure of collagen^{II}.

According to the instructions, 50 µg of protein were taken from each sample and each mixed with 1 ml of the Sircol dye at room temperature for 30 min. Afterwards the samples were centrifuged for 10 min at 10 000 x g. The supernatant including unbound dye was aspirated carefully and 1 ml of Alkali solution was added to the pellet. Alkali solution contains 0.5 M NaOH and dissolves the dye from the dye-collagen-complex. Same procedure was performed with samples of acid soluble collagen type-1 [2.5; 5; 10; 20; 30; 40; 50 µg], which were used to construct a standard curve based on their absorption. Pellets were re-dissolved by vortexing and the samples as well as the collagen standards were transferred to a 96well plate in order to measure their absorption in a spectrophotometer at 540 nm. The calculation of the collagen content was performed via interpolation using the standard curve.

3.2.8 RNA isolation and measurement

Isolation of total RNA from fibroblasts was performed according to the manufacturers' instructions using the RNeasy Mini Kit. Furthermore, during the procedure a recommended DNase digestion was carried out with an RNase free DNase set to avoid any contamination with DNA. The concentration and quality of the obtained RNA was determined by measuring the optical density of the obtained solutions with a Nanodrop ND-100 spectrophotometer.

The wave length for maximal absorption of nucleic acids is 260 nm. Absorption of single stranded (ss) RNA solution at this wave length is 1, when the concentration is 33 µg/ml. This is the so called Optical Density at 260 nm (OD_{260nm}).

Proteins, that often form a contamination source, have an absorption maximum of 280 nm. Hence, by calculating the quotient OD_{260nm}/OD_{280nm} the pureness of the nucleic acid could be assessed. The value should not be below 1.8 to exclude a contamination with proteins. The quotient of a pure RNA solution is 2.0.

3.2.9 cDNA synthesis

To be able to analyze the transcript (mRNA) level by quantitative reverse transcription polymerase chain reaction (qRT-PCR), the RNA was transcribed into complementary cDNA. This process is catalyzed by reverse transcriptase (RT) an RNA-dependent DNA polymerase. The following protocol was used:

500 ng RNA were used and if necessary put to a volume of 10 μ l with RNase free water.

The RNA samples were initially heated to 70 °C in a Thermo Cycler for 10 min. This denaturation step was followed by 5 min of cooling down and centrifugation. Then the Mastermix was added:

<i>Reagent</i>	<i>Volume</i>	<i>Company</i>
10x PCR buffer (without MgCl ₂)	2 μ l	Applied Biosystems, USA
MgCl ₂ (25 mM)	4 μ l	Invitrogen, Germany
dNTPs	1 μ l	Promega, USA
Random Hexamers (50 μ M)	1 μ l	Promega, USA
RNase Inhibitor (20 U/ μ l, 2000 U)	0.5 μ l	Applied Biosystems, USA
Reverse Transcriptase MuLV RT (50 U/ μ l, 5000 U)	1 μ l	Applied Biosystems, USA
ddH ₂ O	0.5 μ l	
Σ 10 μ l + 10 μ l RNA (500 ng)		

The Random Hexamers have a random base sequence and serve as primers that attach to ssRNA. The RT starts to put dNTPs in 5'-3' direction to the strand. The mixtures (20 μ l) were transferred to the Thermo Cycler using the following protocol:

1. Attachment of the Random Hexamers 20 °C for 10 min
2. Reverse Transcription 43 °C for 75 min
3. Inactivation of the Reverse Transcriptase 99 °C for 5 min
4. Cooling 4 °C

Obtained cDNA was stored at -20 °C.

3.2.10 Quantitative reverse transcription polymerase chain reaction (qRT-PCR)

PCR is a method that allows the enzymatic amplification of any DNA/cDNA sequences in order to detect them. Each reaction cycle consists of three steps that run at different

temperatures: 1) denaturation of the DNA sample, 2) hybridisation of the primer oligonucleotides, and 3) elongation of the target sequence by a thermostable DNA-dependent DNA polymerase. In 20-50 of such cycles the desired dsDNA product increases exponentially and can be detected. One entire PCR reaction can be distributed into four phases that refer to the manner of product increase:

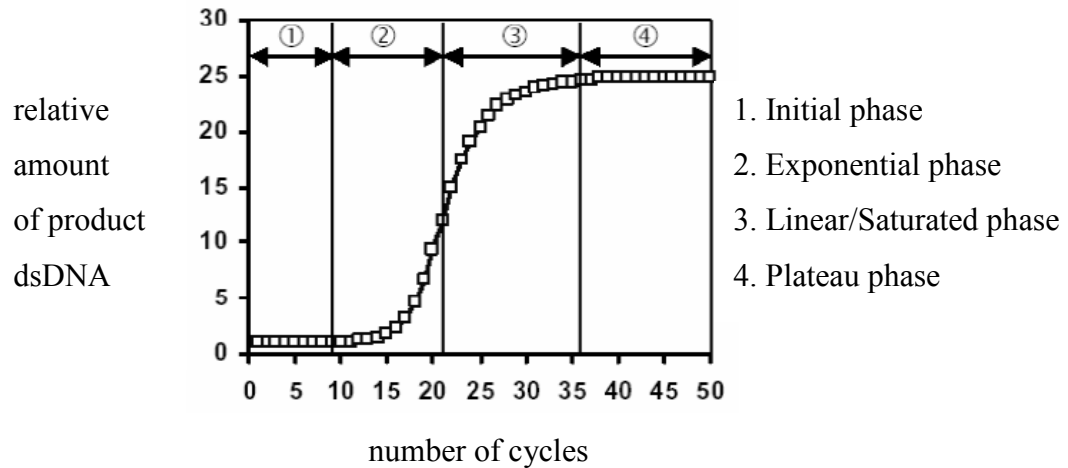


Figure 9. Phases of a PCR reaction

Semiquantitative PCR requires subsequent analysis of the PCR product, so called endpoint analysis. Mostly, the sequences are separated via gelelectrophoresis. During quantitative PCR, however, a simultaneously quantification of the initial amount of the amplified sequence can be performed next to the amplification. Therefore, DNA-specific fluorescence signals are used. Those conduct proportional to the product accumulation and are measured during the reaction and the end of each cycle respectively. Hence, all data are obtained in „real-time“. Additional working steps are not necessary, which decreases the risk of contamination considerably.

3.2.10.1 Measurement of fluorescence with SYBR Green I

One possibility of online-detection is the fluorescence measurement with SYBR Green I, an asymmetric cyanine dye that binds sequence independently to the minor grooves of double stranded (ds) DNA. The emission of fluorescent light of the bound dye increases 1000-fold compared to the free dye. Thus, product (dsDNA) accumulation can be detected by signal increase. This occurs firstly in the hybridisation (annealing) phase, when the primer binds to the ssDNA and steadily increases until the end of the elongation phase. Measurement is

performed at the end of the elongation phase of each cycle because then the amount of dsDNA and therefore also the fluorescence intensity reach their maxima. The occurrence of non-specific products like primerdimers alters the amplification efficiency and thereby causes a systematic quantification error that has to be avoided by optimising the quantitative analysis. In sequence-specific detection methods these non-specific products also occur but are not detected. Thus, with SYBR Green I a further characterization of the used primerset is allowed which the sequence-specific detection is lacking⁷⁸.

3.2.10.2 Primerdesign and efficiency test

Primer sequences were taken from gene bank of the NCBI. The design of the definite primers was carried out with the program primer express 3.0, considering the following criteria as accurately as possible:

- length about 20 – 30 nucleotides to ensure a relatively high annealing temperature.
- almost same frequency of each of the four bases.
- not suitable are regions with particular sequence parts (oligopurine, oligopyrimidin) and regions with pronounced secondary structure.
- avoiding of homo and heterodimeric complementarity at the 3` end that could increase the development of primer dimers.
- optimal annealing temperature: > 45 °C.
- to minimize unspecific binding primers should have strong binding 5` and less strong binding 3` ends.
- melting temperature should be the same for both primers of a pair (forward and reverse).
- Estimation of melting temperature, if number of nucleotides is ≥ 20 : $T_m = [(Number\ of\ A + T) \times 2\ ^\circ C + (Number\ of\ G + C) \times 4\ ^\circ C]$.

For each primer pair the amplification efficiency was determined by serial dilution experiments with at least two dilution steps to cover a high dynamic range. The amplification efficiency should have a value between 1.8 and 2.0.

The primers listed in Table 3 (6.1) were used at a final concentration of 200 nM.

Porphobilinogen deaminase (*Pbgd*), an ubiquitously and constitutively expressed gene in mice cells that is free of pseudogenes, was used as a reference gene in all qRT-PCR reactions.

3.2.10.3 Melting curve analysis

SYBR Green I binds to any dsDNA. A melting curve analysis allows the identification of the PCR product because of temperature-dependent signal decrease as a consequence of the melting of the product. By definition, the melting temperature (T_m) describes the temperature at which half of the DNA is present as a denaturated single strand. T_m is characterized by length and GC content of the dsDNA.

After the 45 PCR cycles, the samples are heated slowly to 90 °C, the products denature at different timepoints and different temperatures, respectively. Melting is accompanied by release of SYBR Green I and thus a rapid decrease of fluorescence. The timepoint of fluorescence decline allows concluding the T_m . Unspecific products, such as primerdimers, are shorter (40 - 45 basepairs (bp)) compared to the amplicon (100 - 200 bp). Thus, they have a lower melting temperature.

In the negative derivative of the melting curve each peak value represents a T_m . As the T_m deviate between specific and non-specific product, the melting curve allows to confirm the amplification of the correct target. Furthermore the area under the curve (AUC) of the maxima is proportional to the product amount ⁷⁸.

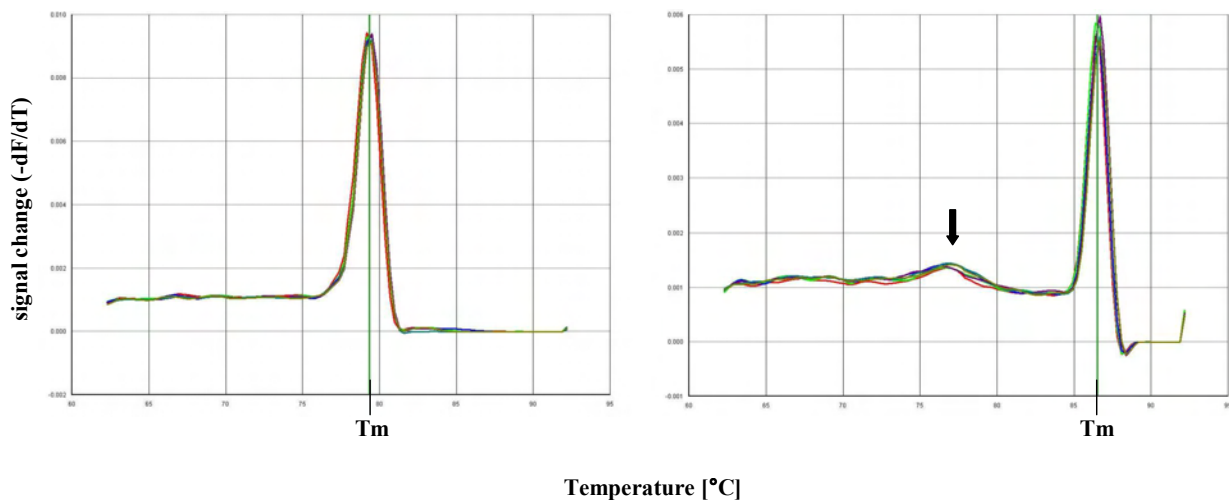


Figure 10. Melting curves

Melting curves of two primersets with different T_m . Detected primerdimers are marked with an arrow.

3.2.10.4 Quantification and analysis of data

To analyze the data, the fluorescence signal is plotted against the number of cycles (amplification plot). The baseline of this graph is determined by the initial phase that corresponds to the cycles in which the fluorescence has not yet started to increase considerably.

The crucial point for quantification is the exponential phase of product accumulation. In this phase, the so-called “threshold” regarding the fluorescence signal has to be assessed. For one gene this value should not change between different samples and runs. The cycle number when the signal reaches this threshold is called Ct (threshold cycle) or crossing point. It depends linear on the logarithm of the initial product concentration and therefore allows its determination. To obtain a relative quantification of the mRNA level of the wanted gene, their Ct values were analyzed as the difference to the reference gene *Pbgd*: $\Delta Ct = Ct_{\text{reference gene}} - Ct_{\text{gene x}}$. Aim of this work was to judge the effects of stimulation on gene expression. Therefore, the relative mRNA level changes of the stimulated samples compared to the unstimulated controls were determined and expressed as $\Delta\Delta Ct$. $\Delta\Delta Ct = \Delta Ct_{\text{stimulated}} - \Delta Ct_{\text{control}}$. The $\Delta\Delta Ct$ corresponds to the binary logarithm of the fold change.

3.2.11 DNA agarose gelelectrophoresis

Agarose gel electrophoresis is a method to separate and visualize DNA fragments according to their size. Negatively charged nucleic acids are moved through the electric field in the gel. The shorter a molecule is, the faster it moves through the gel, what means, that after a certain time period short molecules have covered a longer distance than longer ones. For the 2 % gel, agarose was mixed with 1× TAE buffer. It was additionally supplied with 0.5 µg/µl ethidium bromide (EtBr) to make the fragments visible. EtBr is a dye that intercalates with DNA and fluoresces under ultraviolet light. Before loading onto the gel covered by 1× TAE buffer, the undiluted and 1:10 diluted DNA samples were mixed with 6× DNA loading buffer. Same was performed with the empty control sample. Then electrophoresis was run at 100 V/cm.

3.2.12 Immunofluorescence

Immunofluorescence enables the detection of antigen structures in cells with the help of antibodies. Here, immunofluorescence labeling with fluorochroms was used in order to visualize and localize selectively macromolecules inside the cell. Cells are incubated with a first antibody against the antigen to be analyzed. Next step is the binding of a specific fluorochromalized secondary antibody against the first one. Then the localizations of binding can be observed with a fluorescence microscope. The experiment was performed as following: 15000 fibroblasts per well were plated on special chamber slides. After attachment, synchronisation and stimulation (see above) cells were fixed with acetone/methanol (1:1). To

avoid unspecific binding a blocking step was performed with PBS enriched with 10 % (m/vol) BSA for at least 1 h followed by incubation with the first antibody in accordant dilutions. For secondary binding antibodies were also used in the appropriate dilutions, conjugated with either fluorescein-5-isothiocyanate (FITC) or AlexaFluor. Nuclei were visualized by labeling with 4',6-diamidino-2-phenylindole (DAPI). After incubation, the fibroblasts were fixed with 4 % paraformaldehyde and the slides were covered with DAKO. The fibroblasts were viewed with an immunofluorescence microscope and pictures were taken with a Leica Q Win program.

3.2.13 Statistical analysis

Proliferation assay data were analyzed using the Wilcoxon Rank sum test and the Signed Rank test. All $\Delta\Delta C_t$ values obtained from qRT-PCR and densitometry results from Western Blots were analyzed using the two-tailed, one-sample t-test. All p values obtained from multiple tests were adjusted using the procedure from Benjamini & Hochberg⁷⁹. Results were considered statistically significant when $p < 0.05$ (* $p < 0.05$).

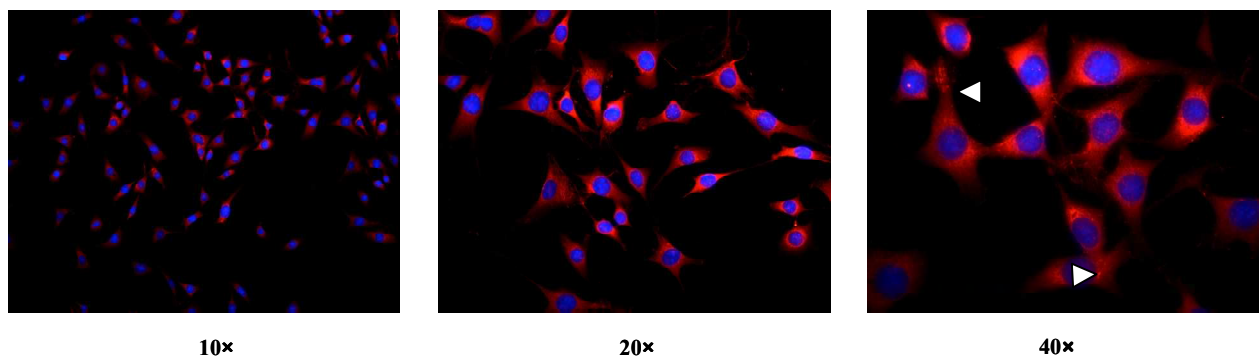
4. Results

4.1 Analysis of occurrence of WNT/ β -catenin signaling in fibroblasts

4.1.1 Phenotype of NIH-3T3 fibroblasts

As a fibroblast cell line NIH-3T3 cells are supposed to produce and secrete collagen. To determine the expression of type I collagen, indirect immunofluorescence was performed with rabbit anti-collagen type 1 antibody (anti-COLT1). In the cytoplasm of almost all fibroblasts collagen expression was observed (Figure 11.A.). Extracellular staining indicated secretion of collagen and thus pointed to its role as extracellular matrix (ECM) component (Figure 11.A. arrows). Alpha smooth muscle actin (α SMA) is known as a (myo-) fibroblast activation marker. In order to ensure that no autoactivation of the cells takes place during culture, expression of this marker was checked with mouse anti- α SMA antibody. Only few cells exhibited SMA expression (Figure 11.B).

A.



B.

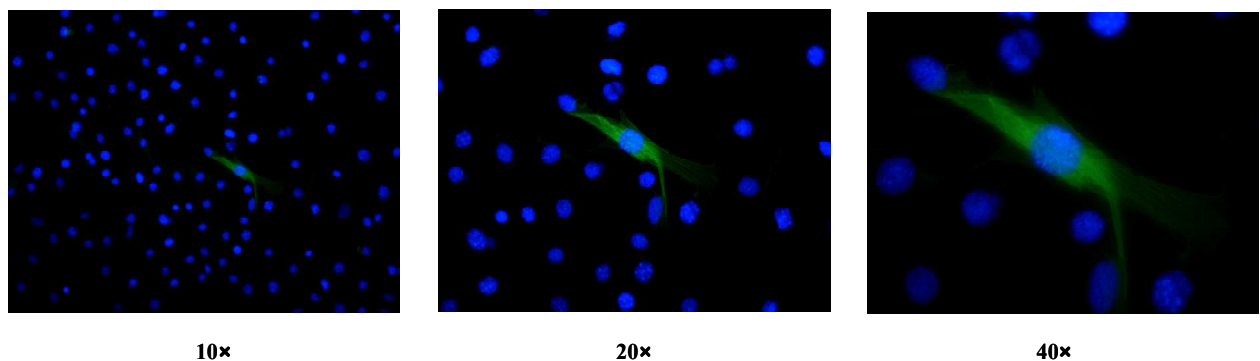


Figure 11. Localization and presence of COLT1 and α SMA in the fibroblast cell line NIH-3T3
(A) Immunofluorescent detection of COLT1 expression with secondary Alexa 555-labelled antibody (red) (original magnification from left to right: 10 \times , 20 \times and 40 \times). Extracellular staining is marked with arrows. (B) Immunofluorescent detection of α SMA with secondary FITC-labelled antibody (green) (original magnification from left to right: 10 \times , 20 \times and 40 \times). Cell nuclei were visualized by DAPI staining (blue). All pictures are representative for at least three independent experiments.

4.1.2 Expression analysis of WNT pathway components in fibroblasts

To investigate, whether WNT signaling can take place in fibroblasts, the expression of WNT pathway components was analyzed. Therefore, the expression of WNT ligands, receptors, coreceptors and intracellular components of the signaling cascade was determined by qRT-PCR. Investigated WNT encoding genes were *Wnt1*, *Wnt3a*, *Wnt8b*, *Wnt10a*, *Wnt10b* and *Wnt11*. On the receptor level primers for Frizzleds (*Fzds*) 1-8 and the coreceptors lipoprotein receptor-related protein (*Lrp*) 5 and 6 were analyzed. Additionally, mRNA levels of the intracellular pathway components β -catenin (*β -cat*) and glycogen synthase kinase (*Gsk*) 3 β , T-cell-specific transcription factor (*Tcf*) 1, 3 and 4 and lymphoid enhancer-binding factor (*Lef*) were assessed (compare dissociation curves in 6.2).

Primer efficiency was determined as indicated in 3.2.10.2. PCR products were visualized by DNA agarose electrophoresis. While the quantification during the PCR run was performed simultaneously to the amplification cycles, the gel electrophoresis formed an endpoint analysis after all 45 cycles. Thus, even for molecules, that are not used for quantification (“not expressed”), product length, as well as melting temperature can be analyzed (compare 6.2, Figure 20). Specific PCR products are shown in Figure 12.A.

To further quantify the gene expression, relative mRNA levels were determined. In Figure 12.B. they are presented as Δ Ct. All WNT ligands were low expressed compared to the reference gene *Pbgd*. *Wnt3a* and *Wnt11* were not expressed (n.e.) at all (Figure 12.B first diagram). On the receptor level, mRNA of all analyzed *Fzds* was present, except of *Fzd6* and *8*. The Δ CT values of *Fzd2* and *7* revealed high expression of these receptors. Same pattern occurred for the coreceptor *Lrp6* (Figure 12.B second diagram). *β -cat* and *Gsk3 β* , key molecules of canonical WNT signaling were highly expressed. Also the presence of transcription factors *Tcf3* and *Tcf4* was observed, whereas *Tcf1* and *Lef1* revealed no or low expression (Figure 12.B third diagram).

A

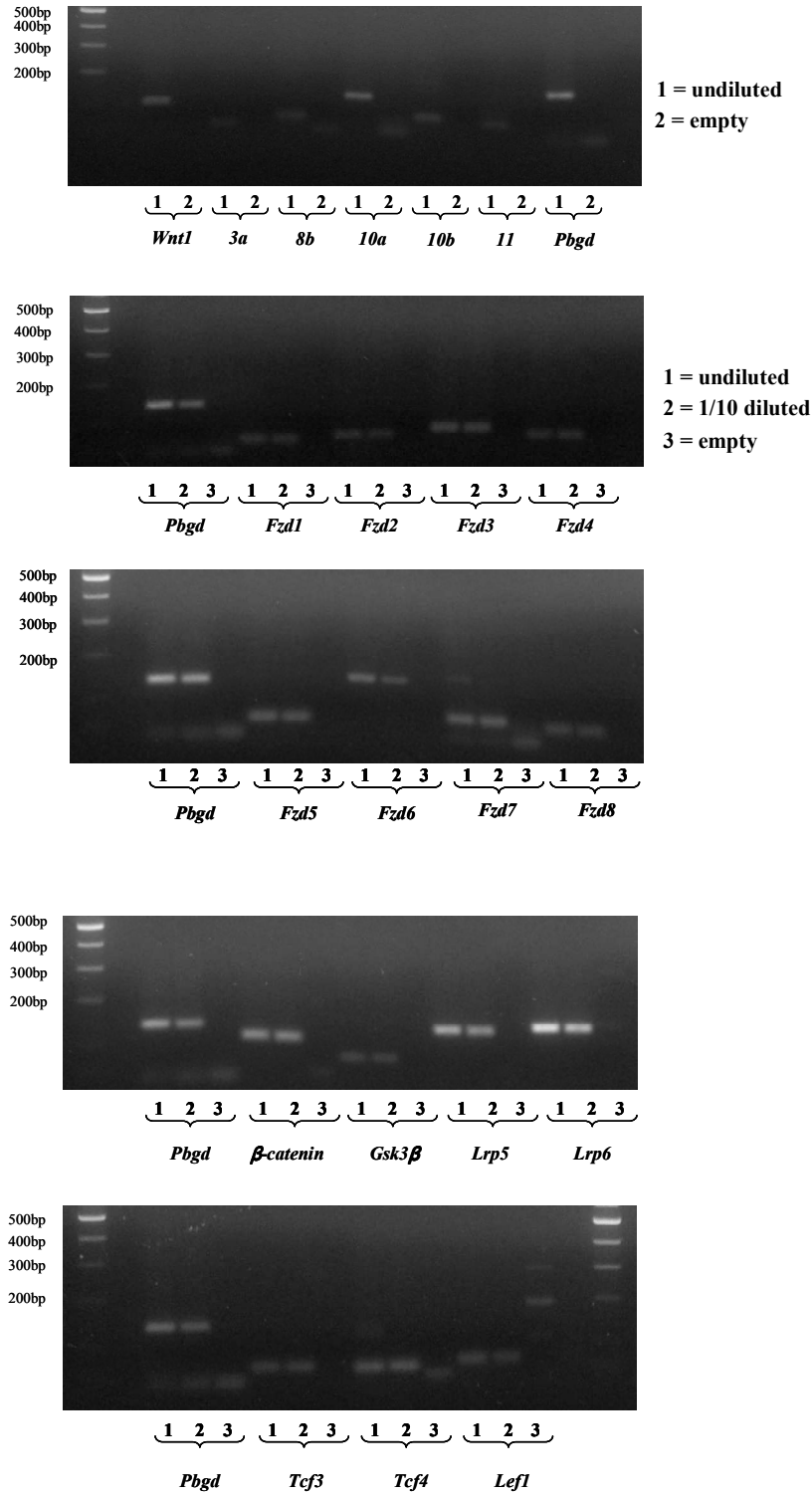


Figure 12. mRNA expression of WNT pathway components in lung fibroblasts
(A) Agarose gel electrophoresis of PCR products. Gels are representative for three independent experiments.

B.

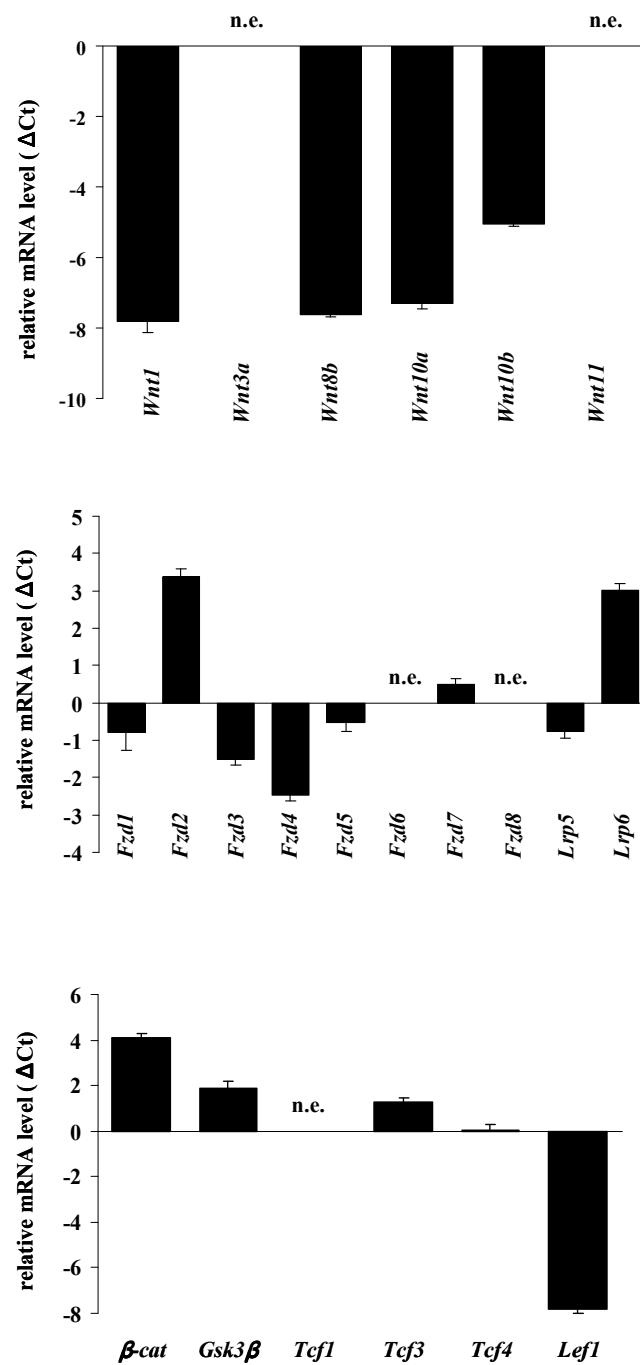


Figure 12. mRNA expression of WNT pathway components in lung fibroblasts

(B) Relative mRNA level of relevant molecules were determined via qRT PCR. *Pbgd* was used as a reference gene. For each pair of primers the ΔC_t value is shown. Expression pattern of WNT ligands, WNT receptors and coreceptors and intracellular components of the pathway.

4.1.3 Induction of WNT/ β -catenin signaling in fibroblasts by stimulation with WNT3a

In order to check if WNT/ β -catenin signaling can be operable in fibroblasts, protein expression of β -catenin (β -CAT) and CyclinD1 (CYCD1), a known target molecule of canonical signaling, was examined via Western blot analysis after stimulation with WNT3a. The blots revealed increased levels of total β -catenin after stimulation for 3, 6, and 12 h (Figure 13.A). These results were confirmed by densitometric analysis. Statistically significant was the upregulation after 6 h (Figure 13.B). CYCD1 protein expression was enhanced as early as 6 h after WNT3a treatment (Figure 13.A).

To further corroborate the activation of the canonical WNT signaling pathway, mRNA level of the known target genes WNT inducible signaling protein (*Wisp*) 1 and *CycD1* were quantified by qRT-PCR. The results of qRT-PCR are presented as mean of $\Delta\Delta C_t \pm$ s.e.m. In accordance to the increasing protein level, the mRNA expression of *CycD1* was increased significantly 6 h after treatment (6 h: 2.75 ± 0.67 , 12 h: 1.71 ± 0.69). (Figure 13.C). Increased expression of *Wisp1* was observed after 12 h (6 h: 1.57 ± 0.94 , 12 h: 1.03 ± 0.26) (Figure 13.C).

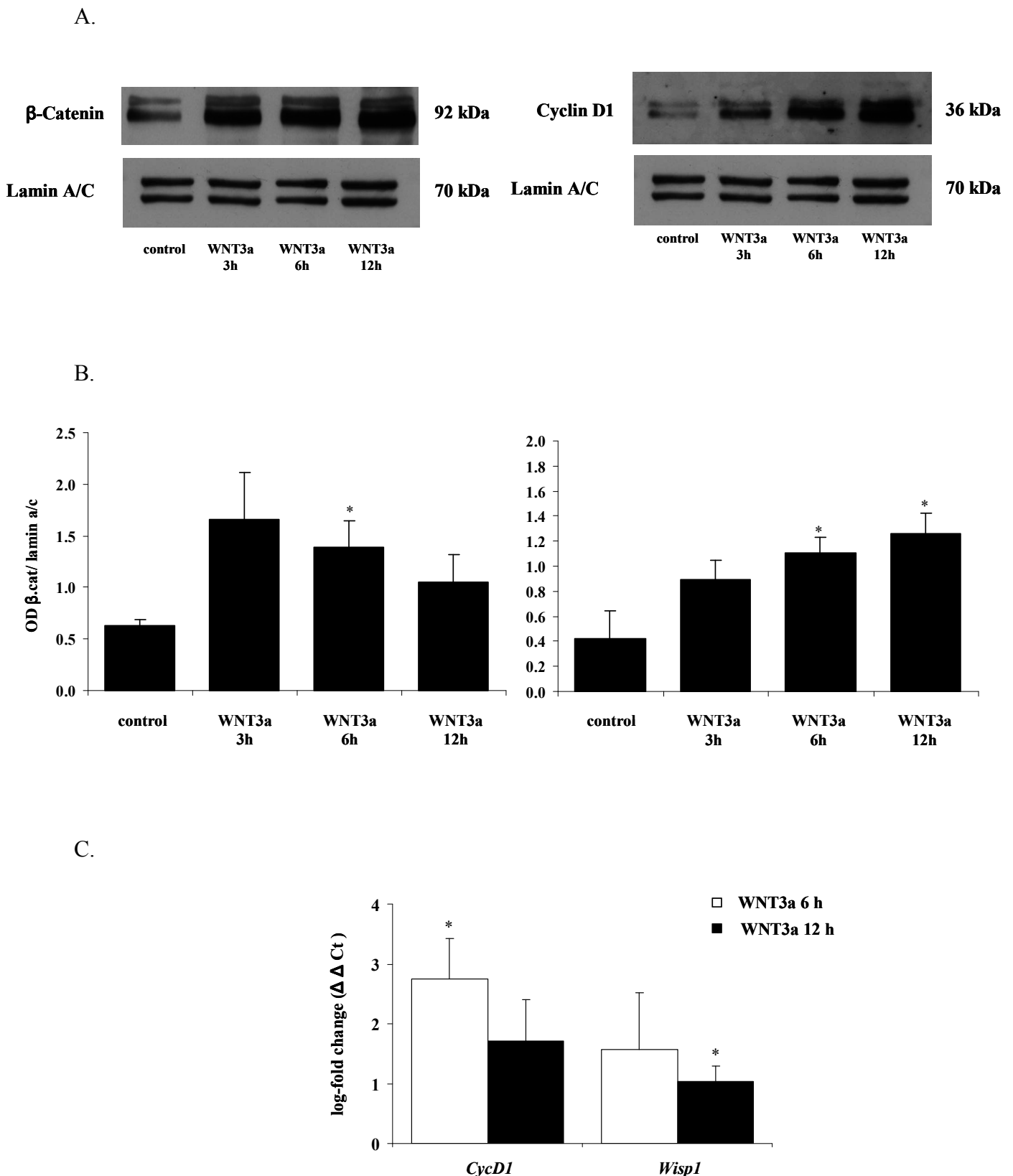


Figure 13. WNT responsiveness of fibroblasts.

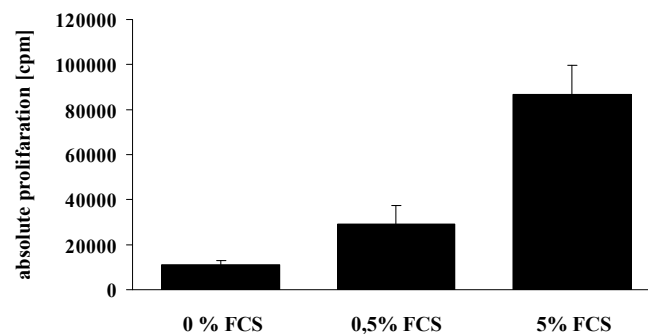
(A) β -Catenin and CYCD1 protein expression levels of control and WNT3a [100 ng/ml]-treated fibroblasts for 3, 6 and 12 h assessed by IB. Lamin a/c served as a protein loading control. Blots are representative for three independent experiments. (B) The results obtained by IB were densitometrically analyzed ($n=3$, $* p < 0.05$), statistical analysis included two-tailed t-test. (C) Fibroblasts were stimulated with WNT3a (100 ng/ml; 6 or 12 h, as indicated mRNA level of WNT target genes *CycD1* and *Wisp1* were determined via qRT-PCR. *Pbgd* was used as a reference gene. Results are presented as mean of $\Delta\Delta Ct \pm s.e.m.$ ($n=3$, $*p < 0.05$).

4.2 Functional analysis of paracrine effects of WNT3a on fibroblasts

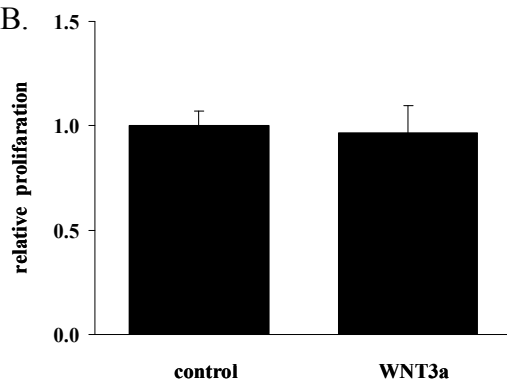
4.2.1 Effects of WNT3a on lung fibroblast proliferation

The WNT/ β -catenin signaling pathway was found to be activated in lung fibroblasts after stimulation with WNT3a (comp. 4.1.3). In order to investigate its functional relevance, potential effects of WNT3a on cell proliferation were analyzed. Cell proliferation was quantified using the ^3H -thymidine proliferation assay. First, fibroblast proliferation due to varying serum conditions was determined. As expected, proliferation of the fibroblasts elevated with increased fetal calf serum (FCS) content (Figure 14.A). Interestingly, fibroblasts stimulated with WNT3a for 20 h in the presence of different concentrations of FCS (0.5 % or 5 % FCS, respectively) did not reveal any significant changes in the proliferation compared with the unstimulated control ($108 \% \pm 13 \%$ and $96 \% \pm 13 \%$, respectively) (Figure 15.B and C).

A.



B.



C.

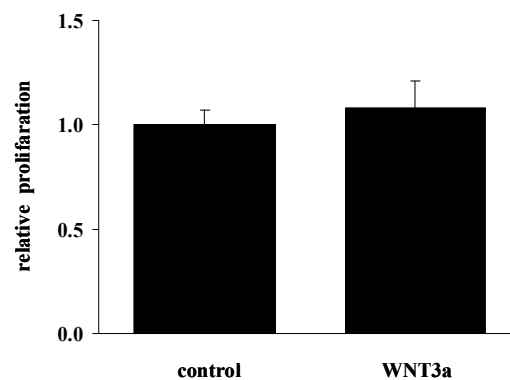


Figure 14. Proliferation of lung fibroblasts after stimulation with WNT3a

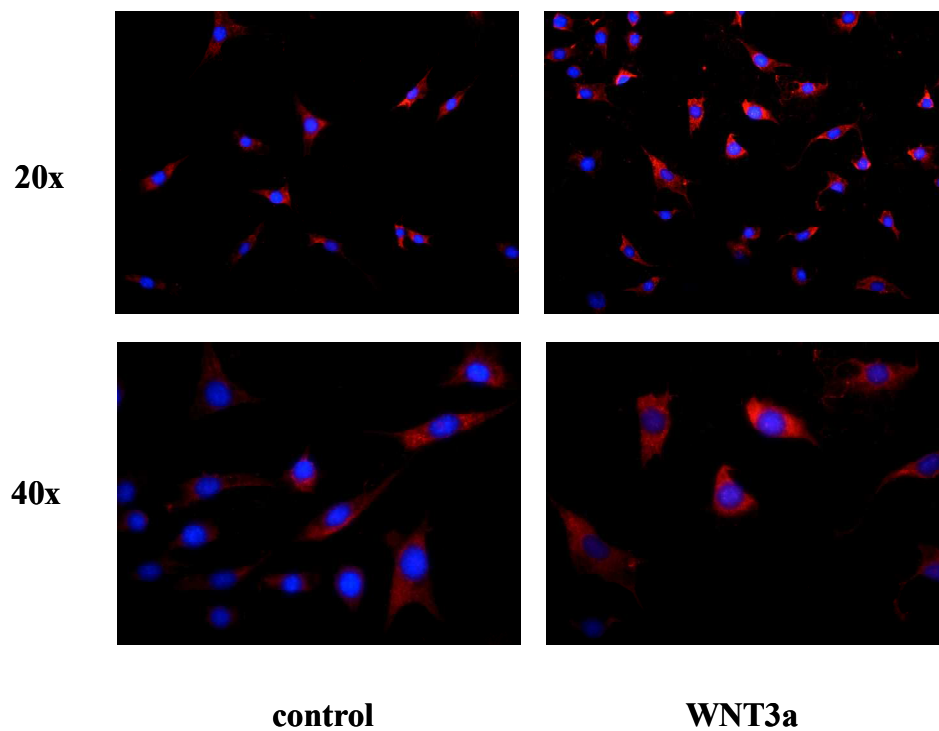
Proliferation of fibroblasts was assessed with ^3H -thymidine proliferation assay. (A) Absolute proliferation [cpm] in different serum conditions. (B) Relative proliferation in medium with 0.5 % FCS after 20 h stimulation with 100 ng/ml WNT3a. Cells from unstimulated medium of the same condition were used as control. (n=3) (C) Relative proliferation in medium with 5 % FCS after 20 h stimulation with 100 ng/ml WNT3a. (n=3)

4.2.2 Effects of WNT3a on collagen deposition of lung fibroblasts

Enhanced extracellular matrix (ECM) deposition and collagen production of activated myofibroblasts is one of the key events in IPF pathogenesis. To examine a potential role of WNT/ β -catenin signaling on this profibrotic processes, the collagen content was determined by immunofluorescence and quantified by Sircol Collagen Assay. For indirect immunofluorescence fibroblasts were stimulated with WNT3a in D-MEM, supplied with 0.5 % or 10 % FCS, respectively. Collagen type I was assessed using a rabbit anti-COLT1 antibody. In both serum conditions, specific collagen expression was observed in the cytoplasm of stimulated and unstimulated fibroblasts (Figure 15.A and B). Cells incubated in 0.5 % FCS generally showed slighter staining (Figure 15.A), whereas 10 % FCS led to a stronger collagen staining in the cytoplasm as well as extracellular, indicating production and secretion of collagen type I by fibroblasts in response to WNT3a (Figure 15. B arrow).

To further quantify the amount of collagen production, the total collagen content was determined using the Sircol Assay. Fibroblasts treated with TGF- β 1, which is a well known mediator of increased collagen production in fibroblasts⁸⁰, were used as a positive control. The whole experiment was performed with fibroblasts in a subconfluent growth stadium (60 %) as well as in almost confluency (90 %). After stimulation with WNT3a at subconfluency, fibroblasts exhibited significant elevation of collagen content about 3 ± 0.4 fold change, while TGF- β 1 stimulated fibroblasts exhibited a 2.5 ± 0.2 fold change (Figure 15.C). Under confluent conditions fibroblasts exhibited a lower increase of collagen content (1.4 ± 0.1 fold for TGF- β 1 and 1.6 ± 0.09 fold for WNT3a) (Figure 15.D).

A.



B.

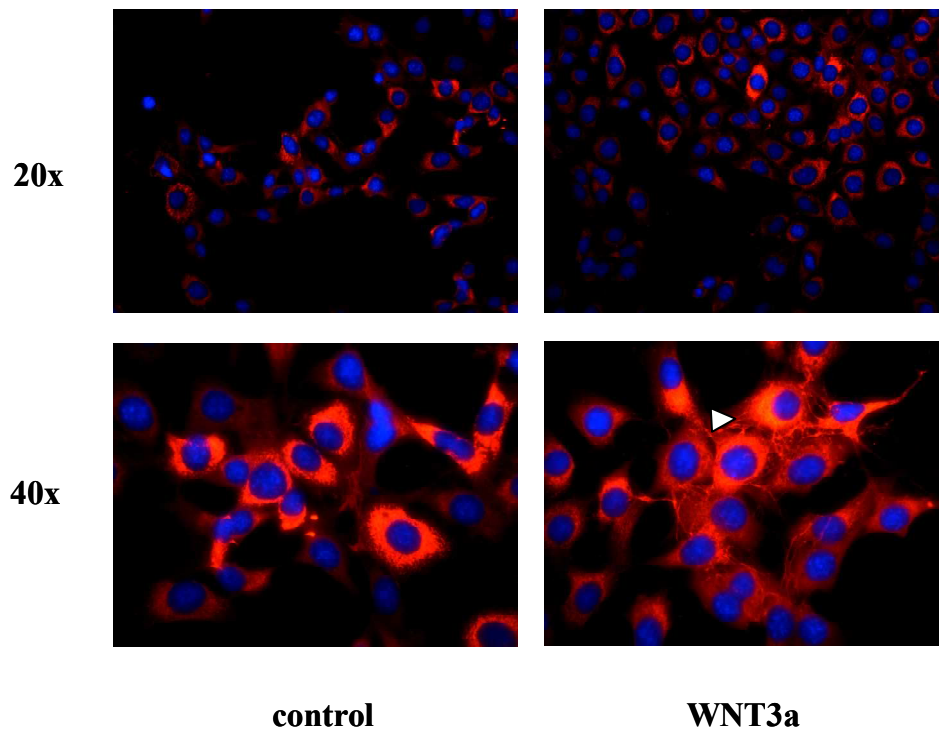


Figure 15. Localization and content of collagen in fibroblasts after stimulation with WNT3a
(A) + (B) Cell nuclei were visualized by DAPI staining (blue). Immunofluorescent detection of COLT1 expression with secondary Alexa 555-labelled antibody (red) (original magnification upper row: 20 \times , lower row: 40 \times). (A) COLT1 staining after stimulation with WNT3a in medium with 0.5 % FCS. (B) COLT1 staining after stimulation with WNT3a in medium with 10 % FCS. All pictures are representative for three independent experiments. Extracellular staining is marked with arrows.

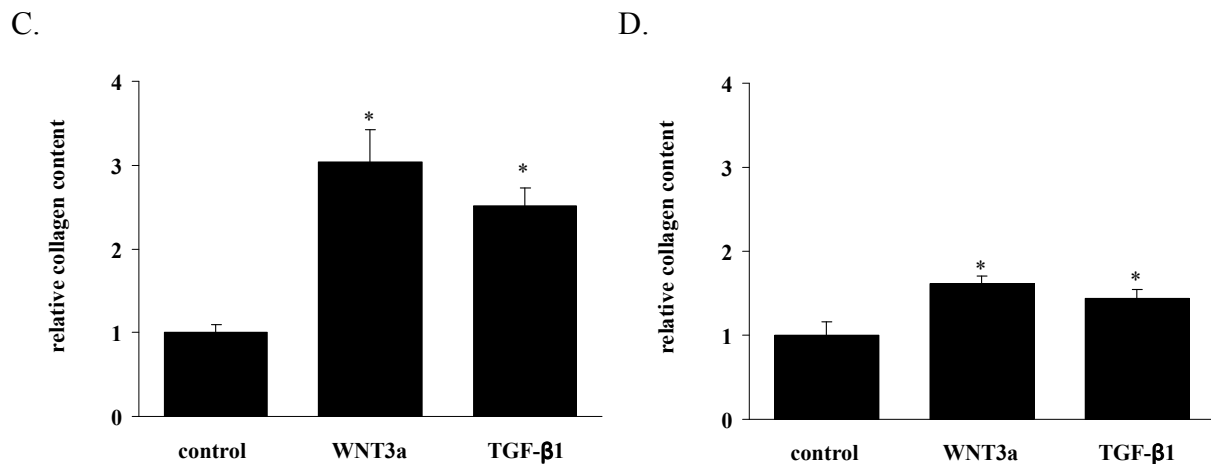


Figure 15. Localization and content of collagen in fibroblasts after stimulation with WNT3a
 (C) + (D) Collagen content of fibroblasts after stimulation with 100 ng/ml of WNT3a was determined with Sircol Assay and is shown relative to the unstimulated control. TGF-β1 stimulated cells were used as a positive control. (n=3, *p< 0.05) (C) Changes in collagen content of fibroblasts that were stimulated in a subconfluent stadium. (D) Changes in collagen content of fibroblasts that were stimulated in almost confluent stadium.

4.2.3 Effects of WNT3a on gene expression of ECM molecules and (myo-) fibroblast markers

Enhanced collagen production of fibroblasts after WNT3a stimulation had suggested profibrotic effects of WNT/β-catenin signaling on fibroblasts. To further confirm these effects and reveal other potential pathomechanisms, the mRNA level of different profibrotic marker genes were analyzed using qRT-PCR after WNT3a treatment for 6 and 12 h. Interestingly, the expression of type I collagen alpha 1 (*Colla1*) and type I collagen alpha 2 (*Colla2*) was not significantly altered after stimulation (mean of $\Delta\Delta\text{CT} \pm \text{s.e.m.}$: *Colla1* 6 h: -0.28 ± 0.11 , 12 h: -0.76 ± 0.32 , Figure 16.A). In addition, the expression of the glycoprotein fibronectin1 (*Fnl1*), an ECM component that plays a role in stabilizing the attachment of the ECM, was not significantly affected by WNT3a treatment (6 h: 0.76 ± 0.71 , 12 h: -0.82 ± 0.14).

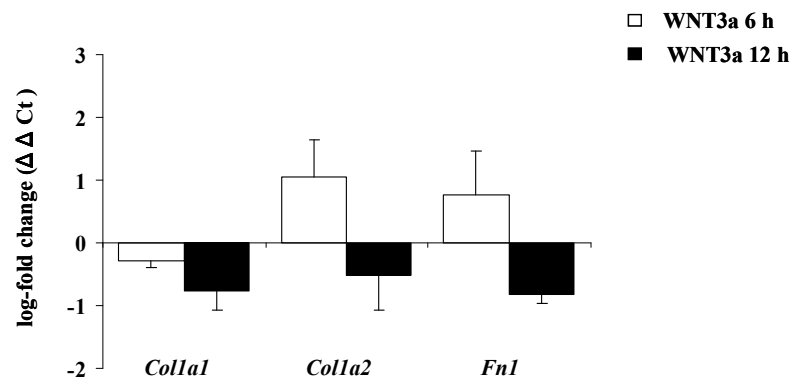
In contrast, a significant increase of the (myo-) fibroblast activation marker alpha smooth muscle actin (*αSma*) was observed after 6 h stimulation (6 h: 0.9 ± 0.17 , 12 h: 0.64 ± 0.3). Additional fibroblast markers, such as the fibroblast specific protein 1 (*Fsp1*), also known as S100a4, and Vimentin were not differently expressed (6 h: 1.09 ± 0.83 , 12 h: -0.33 ± 0.65 and 6 h: -0.32 ± 0.34 , 12 h: 0.04 ± 0.37 respectively, Figure 16.B).

The cytokine transforming growth factor (TGF) -β is already known to play a role in IPF pathogenesis. It can act in a profibrotic way by driving EMT, fibroblast activation, and induction of ECM production ²⁶.

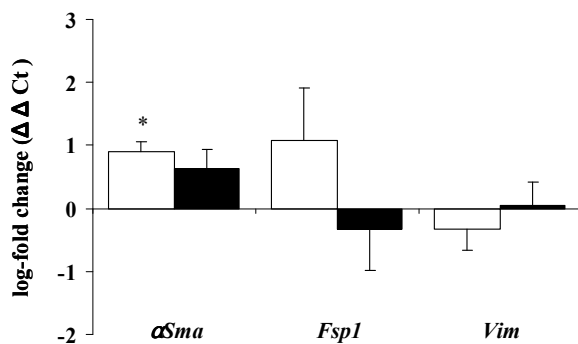
To analyze a possible crosstalk between WNT and TGF- β signaling the effects of WNT treatment on the expression of *Tgfb-1* were checked additionally. Neither after 6 nor after 12 h significant changes were observed (6 h: 0.22 ± 0.82 , 12 h: 0.25 ± 0.12 , Figure 16.C). Furthermore, the expression of arginase (*Arg*) 1 and 2 was examined, as arginase mediates collagen deposition in lung fibrosis⁸¹. Therefore a responsibility for the collagen increase on protein level after WNT3a treatment can be suggested. Both enzymes were not affected significantly after stimulation (6 h: -1.53 ± 0.91 , 12 h: -0.83 ± 0.67 and 6 h: 0.12 ± 0.89 , 12 h: -0.96 ± 0.96 respectively, Figure 16.C).

Taken together, these results revealed that WNT can contribute to fibroblast activation and is a potent inducer of collagen in fibroblasts, however our analysis thus far suggests that WNT signaling does not interfere directly with the transcriptional regulation of collagens.

A.



B.



C.

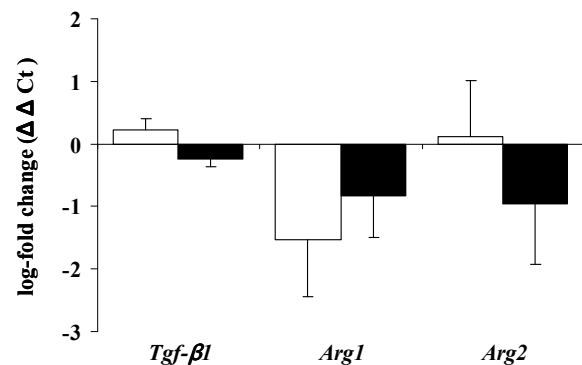


Figure 16. mRNA level of ECM molecules and (myo-) fibroblast markers after stimulation with WNT3a Fibroblasts were stimulated with WNT3a (100 ng/ml; 6 or 12 h, as indicated), and the mRNA levels of different ECM components or (myo-) fibroblast activation markers were analyzed by qRT-PCR (n=4). Results are presented as mean of $\Delta\Delta Ct \pm$ s.e.m., * $p < 0.05$. (A) $\Delta\Delta Ct$ of ECM components. (B) $\Delta\Delta Ct$ of (myo-) fibroblast markers. (C) $\Delta\Delta Ct$ of possible crosstalk partners.

4.3 Functional Analysis of effects of WISP1 on fibroblasts

The WNT1-inducible signaling protein (WISP) 1 is encoded by a target gene of WNT/ β -catenin signaling. In our laboratory high secretion of WISP1 by distorted ATII cells of IPF lungs has already been observed. To analyze, if WISP is a mediator for the reported WNT effects, the effects of WISP1 treatment on fibroblast proliferation, collagen content and marker gene expression were investigated, similar to the approaches described above.

4.3.1 Effects of WISP1 on fibroblast proliferation

Cell proliferation was assessed using the $^3\text{[H]}$ -thymidine proliferation assay. Fibroblasts stimulated with WISP1 in medium either supplied with 0.5 % or 5 % FCS for 20 h did not reveal significant changes in the proliferation compared to the respective control ($89\% \pm 8\%$ and $105\% \pm 9\%$, respectively). (Figure 17.A and B).

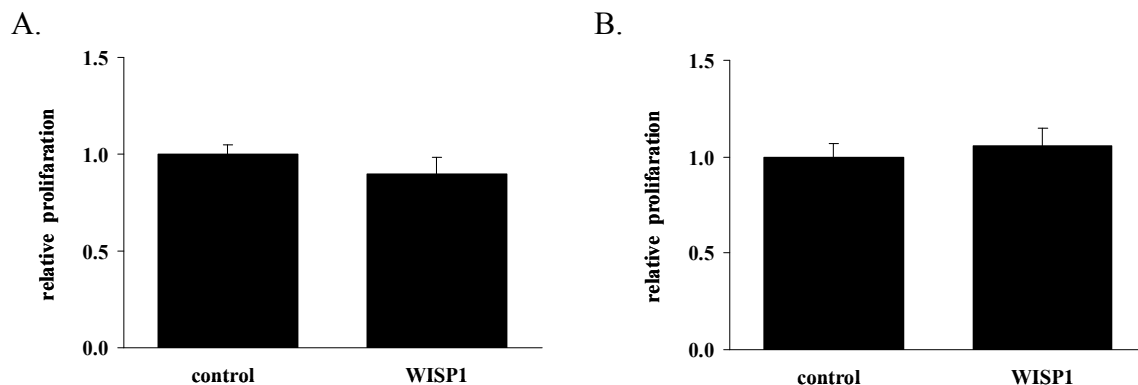


Figure 17. Proliferation of lung fibroblasts after stimulation with WISP1

Proliferation of fibroblasts was assessed with $^3\text{[H]}$ -thymidine proliferation assay. (n=3) (A) Relative proliferation in medium with 0.5 % FCS after 20 h stimulation with 1 $\mu\text{g/ml}$ WISP1. (B) Relative proliferation with 5 % FCS after 20 h stimulation with 1 $\mu\text{g/ml}$ WISP1.

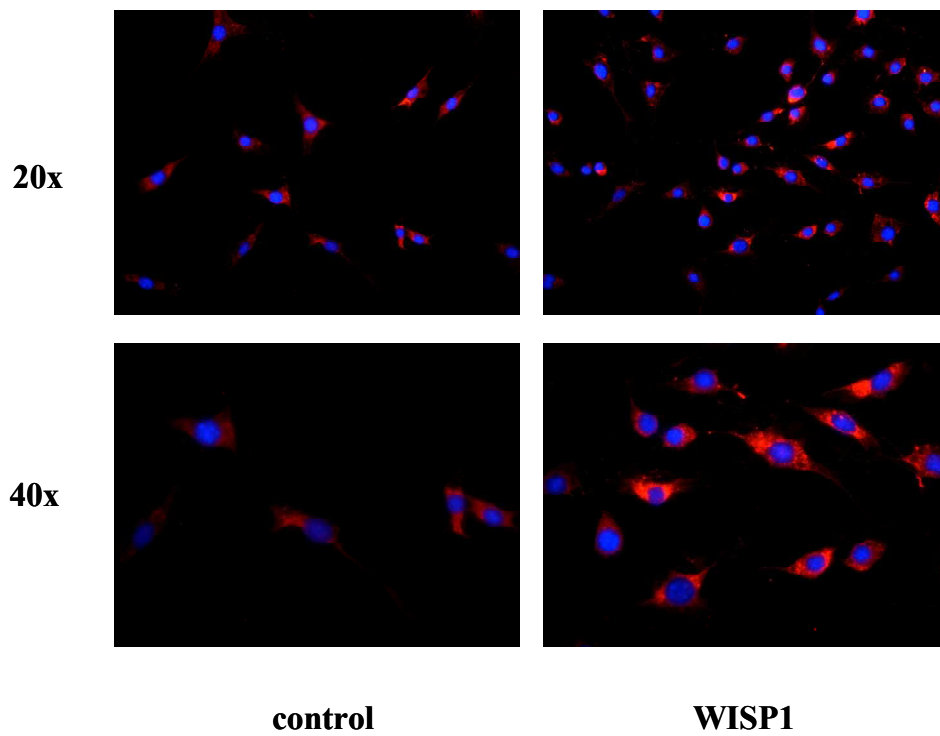
4.3.2 Effects of WISP1 on collagen deposition of fibroblasts

To analyze WISP1 effect on matrix deposition during IPF, collagen deposition of fibroblasts was assessed after stimulation with WISP1. Immunofluorescence and Sircol Collagen Assay were performed to determine and quantify collagen content in the fibroblasts, respectively.

For indirect immunofluorescence fibroblasts were stimulated with WISP1 in D-MEM, supplied with 0.5 % or 10 % FCS, respectively. Collagen type I was assessed using a rabbit anti-COLT1 antibody. In both serum conditions, specific collagen expression was observed in the cytoplasm of the fibroblasts, similar to the localization patterns in 4.2.2. Stimulated cells exhibited specific collagen staining in the cytoplasm (Figure 18.A+B). The staining after incubation in 0.5 % FCS–medium was slighter than in 10 %. But in both serum conditions, control and WISP1 stimulated cells exhibited distinct cytoplasmic and extracellular (arrow) collagen staining pattern (Figure 18.A+B).

To determine collagen quantity in the fibroblasts after WISP1 treatment, Sircol Collagen Assay was performed. The collagen content was determined 20 h after stimulation with WISP1. Fibroblasts stimulated with TGF- β 1 were used as a positive control. The whole experiment was performed with fibroblasts in a subconfluent growth stadium (60 %) and in almost confluency (90 %). After stimulation with WISP1 at subconfluency, fibroblasts exhibited significant elevation of collagen content about 2.4 ± 0.1 fold change (Figure 18.C). Under confluent conditions, fibroblasts revealed significant increases of collagen content of 1.5 ± 0.2 fold change after stimulation with WISP1 (Figure 18.D).

A



B.

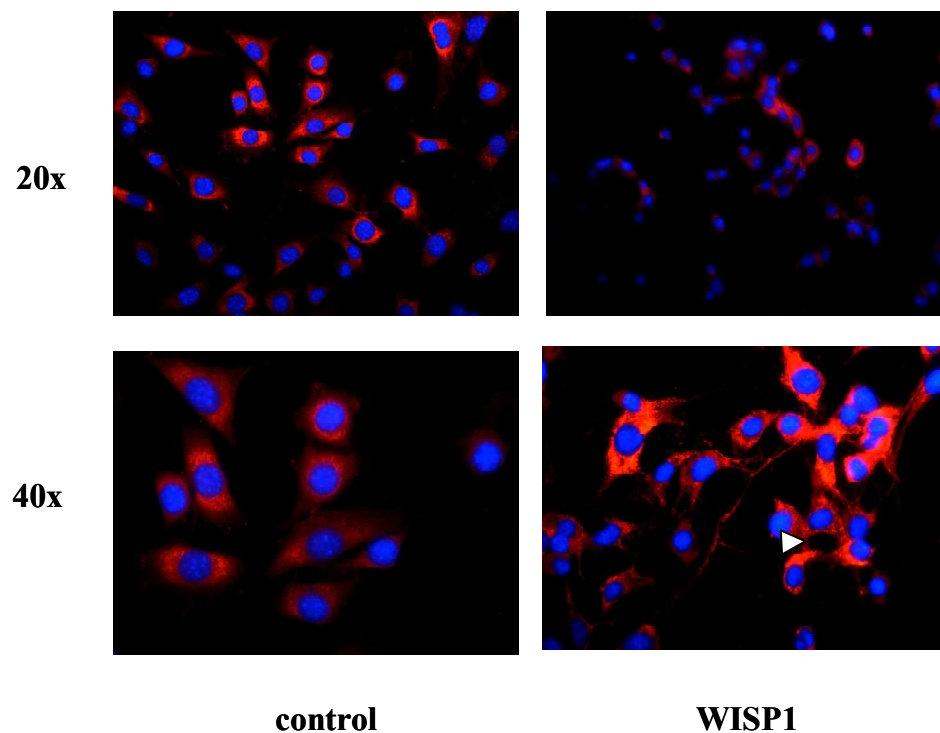


Figure 18. Localization and content of collagen in lung fibroblasts after stimulation with WISP1
(A) + (B) Cell nuclei were visualized by DAPI staining (blue). Immunofluorescent detection of COLT1 expression with secondary Alexa 555-labelled antibody (red) (original magnification upper row: 20 \times , lower row: 40 \times). (A) COLT1 staining after stimulation with WISP1 in medium with 0.5 % FCS. (B) COLT1 staining after stimulation with WISP1 in medium with 10 % FCS. All pictures are representative of three independent experiments. Extracellular staining is marked with arrows.

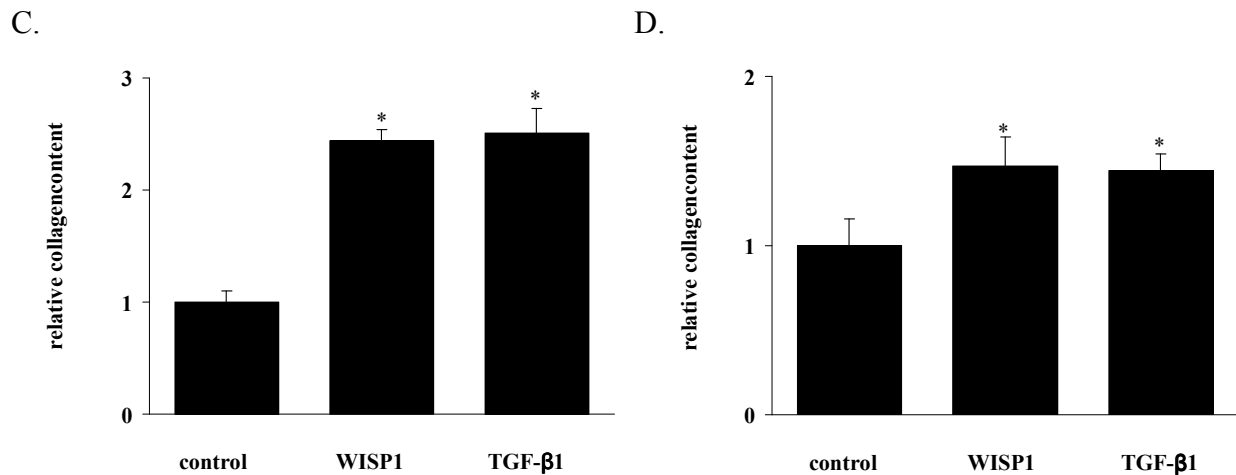


Figure 18. Localization and content of collagen in lung fibroblasts after stimulation with WISP1
 (C) + (D) Collagen content of fibroblasts after stimulation with 1 $\mu\text{g/ml}$ of WISP1 was determined with Sircol Assay and is shown relative to the unstimulated control. TGF- β 1 stimulated cells were used as a positive control. (n=3, *p< 0.05) (C) Changes in collagen content of fibroblasts that were stimulated in a subconfluent stadium. (D) Changes in collagen content of fibroblasts that were stimulated in almost confluent stadium.

4.3.3 Effects of WISP1 on gene expression of ECM molecules and (myo-) fibroblast markers

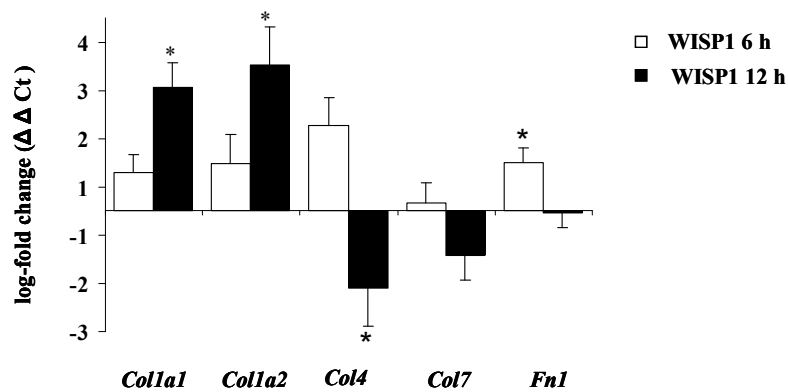
Enhanced collagen content in fibroblasts after stimulation with WISP1 as well as its upstream molecule WNT3a had indicated profibrotic effects of the pathway on fibroblasts. To investigate if WISP1 acts as a mediator leading to fibroblast activation and collagen transcript expression, different genes were analyzed using qRT-PCR after WISP1 treatment for 6 and 12 h, as described above after WNT3a stimulation. The results of qRT-PCR are presented as mean of $\Delta\Delta\text{Ct} \pm \text{s.e.m.}$ Following factors belonging to the ECM were determined: *Colla1*, *Colla2*, collagen 4 (*Col4*), collagen 7 (*Col7*) and *Fnl*. *Colla1* and *Colla2* were regulated by WISP1 (Figure 19.A). After 12 h significant increase of the expression of both could be observed: $\Delta\Delta\text{Ct} \pm \text{s.e.m.}$ of 2.5 ± 0.52 for *Colla1* and 3.02 ± 0.82 for *Colla2*. Interestingly, *Col4* expression was enhanced after 6 h (6 h: 1.76 ± 0.6), but significantly downregulated after 12 h (12 h; -1.61 ± 0.78). *Col7* was generally low expressed in the fibroblasts (ΔCT not shown) and not altered significantly (6 h: 0.18 ± 0.42 , 12 h: -0.93 ± 0.51). *Fnl* expression exhibited a significant increase after 6 h of stimulation, whereas after 12 h no changes were observed (6 h: 1.02 ± 0.29 , 12 h: -0.05 ± 0.3 , Figure 19.A). Next, a possible influence of WISP1 on fibroblast activation was checked by examining the expression levels of typical (myo-) fibroblast activation markers. The expression of *αSma* was increased significantly after 6 h stimulation (6 h: 0.62 ± 0.09 , 12 h: 0.15 ± 0.22). *Fsp1* expression was enhanced at

both timepoints (6 h: 0.46 ± 0.18 , 12 h: 0.67 ± 0.23). The mRNA level of *Vim* were not changed (6 h: -0.36 ± 0.31 , 12 h: -0.07 ± 0.35 , Figure 19.B).

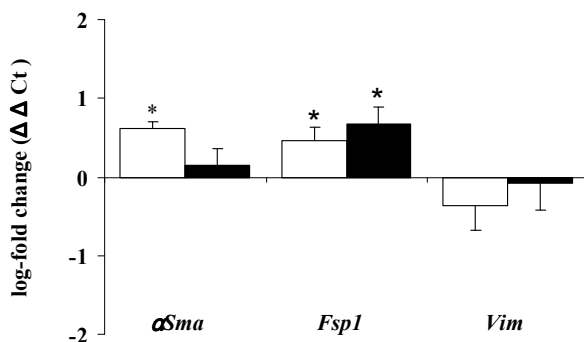
Next to the crucial role of the TGF- β system in IPF²⁶, a role of Plasminogen activator inhibitor (PAI) -1 was already reported⁸². To reveal possible crosstalks to these signaling pathways, expression of *Pai1* and *Tgf- β 1* in fibroblasts was analyzed after stimulation with WISP1. *Pai1* was upregulated after 12 h (6 h: -0.91 ± 0.09 , 12 h: 0.96 ± 0.47), whereas *TGF- β 1* was not altered on mRNA level after WISP1 treatment (6 h: 0.04 ± 0.22 , 12 h: -0.08 ± 0.09 , Figure 19.C).

In summary, our results revealed that WISP1 can induce collagen expression in fibroblasts on transcriptional and protein level. Furthermore, it led to an increased expression of ECM components and (myo-) fibroblast activation markers.

A.



B.



C.

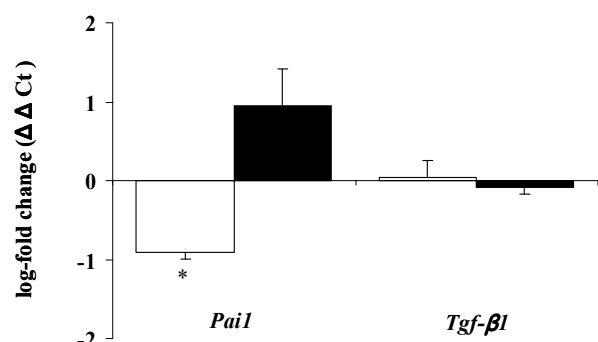


Figure 1. mRNA level of ECM molecules and fibroblast markers after stimulation with WISP1

Fibroblasts were stimulated with WISP1 (1 μ g/ml; 6 or 12 h, as indicated), and the mRNA levels of different ECM components or (myo-) fibroblast activation markers were analyzed by qRT-PCR (n=4). Results are presented as mean of $\Delta\Delta\text{CT} \pm \text{s.e.m.}$, * $p < 0.05$.

(A) $\Delta\Delta\text{CT}$ of ECM components. (B) $\Delta\Delta\text{CT}$ of (myo-) fibroblast markers. (C) $\Delta\Delta\text{CT}$ of possible crosstalk partners.

5. Discussion

5.1. Fibroblasts in IPF pathogenesis

Idiopathic pulmonary fibrosis (IPF) represents the most common and most severe form of the idiopathic interstitial pneumonias (IIP). In spite of extensive research on the field, the pathomechanisms are still not understood. Refractory to medicamentous therapy the disease rapidly leads to the death of the patient because of respiratory failure.

The initiation of the disease currently is ascribed to alveolar epithelial cell injury and subsequent inadequate repairmechanisms^{2,7,18}.

In the present study fibroblasts as key effector cells in the pathogenesis of IPF were in the focus of our research. Being activated to myofibroblasts and forming fibroblast foci that are responsible for an extensive collagen-rich extracellular matrix accumulation in the interstitium of the lung, fibroblasts are considered as triggers for the progression of the disease^{26,27}. However, the origin of these fibroblasts remains unclear. As one possible origin for the fibroblasts, bone marrow-derived fibrocytes are discussed⁸³. Circulating to the lung during fibrosis, they could serve as precursors for the interstitial fibroblasts⁸⁴⁻⁸⁶. A second theory claims epithelial-to-mesenchymal transition (EMT) being the source of the fibroblasts. It includes a phenotypic switch of epithelial to fibroblast-like cells, subsequently to changes in gene and protein expression of ATII cells⁸⁷⁻⁸⁹.

Thirdly, a possible role of local growth factors and cytokines triggering the activation and differentiation of the fibroblasts is well accepted^{8,28,90}. Source of profibrotic molecules are probably hyperplastic ATII cells that are known to express growth factors like transforming growth factor- β 1 (TGF- β 1), platelet derived growth factor (PDGF), and the cytokine tumor necrosis factor- α (TNF- α)^{7,12}. TGF- β 1 as one example has profibrotic effects in human lung fibroblasts, inducing an altered secretion of collagens and total ECM and thereby influencing the pathogenesis of IPF^{26,80}.

The present report was focused on the third theory by analysing possible trigger molecules that could have paracrine effects on lung fibroblasts and thereby contribute to the development of the fibroblast phenotype that is found in IPF.

5.2. WNT/ β -catenin signaling in lung fibroblasts

In regard to the pathophysiological mechanisms of IPF progression, the WNT/ β -catenin system is of particular interest. On the one hand, a role of WNT/ β -catenin signaling in different diseases is well established. On the other hand, presence of WNT in the respiratory system can be stated. It is functionally involved in lung development as well as in lung cancer^{31,35,50,51,91}. Increased WNT/ β -catenin signaling in IPF was reported by Chilosi et al. (2003)⁶¹ and recently by our group^{62,77}.

WNT/ β -catenin signaling is neither limited to a special tissue nor to a cell type. Actually, the functional response differs cell type specific³⁵. Therefore in every tissue and organ it is important to examine different cell types and their affection by WNT signaling separately. This project focused on lung fibroblasts and their relation to WNT/ β -catenin signaling in IPF. Several reports deal with WNT/ β -catenin signaling in fibroblasts. Recently, WNT responsiveness and induction of already known and also new target genes in human fibroblasts were described⁹². In their publication about aberrant WNT/ β -catenin pathway activation in IPF, Chilosi and colleagues (2003) reported nuclear β -catenin accumulation in fibroblasts based on immunohistochemical observations⁶¹. Thus, the conclusion stands to reason that lung fibroblasts constitute WNT target cells in association with IPF. This was recently emphasized by our report about functional WNT signaling in IPF that examines cell-specific expression patterns of WNT ligands and pathway components⁶². Although receptors and intracellular signal transducers of the WNT/ β -catenin pathway mainly localize in the bronchial and alveolar epithelium, primary human fibroblasts also exhibited presence of these pathway components. These observations underline the suggestion that paracrine extracellular WNT binding can activate the downstream signaling pathway inside the cell.

Additionally to the expression and localization analysis, an increased phosphorylation of WNT signal transducing molecules in IPF was observed⁶², which is the most sensitive indicator of WNT activity in tissue sections^{62,93,94}.

In the present project experiments were performed with mouse fibroblasts. Expression analysis of WNT ligands and WNT/ β -catenin pathway components did not suggest WNT secretion by fibroblasts, but responsiveness to extracellular paracrine ligand binding on the cells. This was further confirmed by an increase of intracellular total β -catenin, the key molecule of the signaling pathway, after stimulation with WNT3a, a known inducer of WNT/ β -catenin signaling. Accumulation of β -catenin is a consequence of dephosphorylation, which requires an activated WNT/ β -catenin pathway. Significant elevation, of the WNT

target molecule and cell cycle regulator Cyclin (CYC) D1 was another finding that indicated active WNT signaling. The occurring double band of CYCD1 might be due to posttranslational modification, like phosphorylation, which is known to regulate presence, localization, and activity of CYCD1 inside the cell⁹⁵. In accordance to the protein increase, the mRNA level of *CycD1* was significantly upregulated after 6 h of stimulation. Pathway activation was further confirmed by upregulation of *Wisp1*, another known target gene⁶⁵, after 12 h of stimulation with WNT3a.

Having shown that the WNT/ β -catenin signaling pathway can be activated in lung fibroblasts by stimulation with WNT3a, the functional relevance thereof was analyzed considering the hypothesis of WNT3a having profibrotic effects .

In particular, changes in proliferation, collagen deposition and marker gene expression after stimulation with WNT3a were investigated.

Concerning proliferation, descriptions of fibroblast phenotypes in pulmonary fibrosis differ in literature. High proliferation rates are reported as well as low rates. This diversity may be related to different states of the disease, as reviewed by Selman et al. (2001) who assume a phenotypic change of fibroblasts in the course of the disease from a first migratory, then proliferative and finally synthetically active type⁷. Latter exhibit the typical myofibroblast characteristics that are contractility and abundant production of extracellular matrix components²⁵. In this phenotype proliferation takes a back seat, what stands in accordance to the observation that more advanced fibrosis is associated to low fibroblast proliferation rates⁹⁶. In the present report fibroblast proliferation was checked after stimulation with WNT3a in different serum conditions. Proliferation was not affected after stimulation with WNT3a. The lacking proliferation change in 5 % could be referred to an already maximal proliferation due to the overabundance of nutrients by the serum. However, in 0.5 % a definite capacity for the cells to proliferate is left (compare Figure 14.A). The observation that this is not induced by stimulation with WNT3a leads to the conclusion that activated WNT/ β -catenin signaling *in vitro* does not have direct proproliferative effects on fibroblasts. In contrast, the non canonical ligand WNT5a in a recent study revealed proproliferative effects on fibroblasts⁹⁷.

At this point in time the lacking influence on proliferation did not allow excluding the contribution of paracrine canonical WNT effects to the synthetic activation of the fibroblasts. In fact, there are several reports that claim the synthetic activity of fibroblasts in IPF being more emphasized than the proliferation capacity. Raghu et al. (1988)⁹⁶ and Hetzel et al. (2005)⁹⁸ observed higher proliferation rates in normal fibroblasts in response to growth factor

stimulation, whereas IPF fibroblasts exhibited enhanced synthetic activity.

To analyze alteration of the synthetic activity of the fibroblasts by WNT3a or WISP, collagen content as a representative ECM component that is expressed and secreted by fibroblasts was determined. Before its secretion into the interstitium, procollagen undergoes a large number of posttranslational modifications⁹⁹. Immunofluorescence staining of stimulated as well as unstimulated cells demonstrated that cultured fibroblasts in general produce collagen and contain it in their cytoplasm. Staining between the cells indicated secretion of the protein reflecting *in vivo* processes of ECM formation⁹⁹. However, stainings did not allow quantifying a difference between collagen amount of unstimulated and stimulated fibroblasts. Thus, quantitative collagen measurement was performed. The presented data reveal the ability of active WNT signaling to increase collagen content in fibroblasts, suggesting an activation of *de novo* collagen synthesis by the ligand. These findings could deliver an explanation for the lacking effects on proliferation. Rhudy et al. (1988) reported that fibrillar collagen, which is the natural form of type I collagen, acts as a negative regulator on fibroblast proliferation¹⁰⁰.

Actually, for IPF these results indicate a contribution of WNT in a profibrotic manner as *de novo* ECM/collagen synthesis and deposition by fibroblasts represent a characteristic trigger of fibrosis⁸⁰. This is underlined by the observation that WNT induced collagen increase exceeds the one caused by TGF- β 1, which was used as a positive control.

However, it has to be respected that increased collagen production is not necessarily followed by increased ECM secretion. Regarding this, it would be interesting to assess ECM/collagen secretion of lung fibroblasts after WNT stimulation by supernatant analysis. To confirm the results and further quantify the collagen amount, Hydroxyprolin assay could be performed.

While overexpression of WNT target genes in IPF lungs has already been revealed by unbiased microarray screens^{64,101,102}, the present report aimed to analyze the functional relevance of active WNT/ β -catenin signaling. Either ECM components or myofibroblast marker encoding genes were chosen to be analyzed by quantitative RT-PCR after stimulation with WNT3a. Interestingly, for type I collagen α 1 (*Colla1*) and type I collagen α 2 (*Colla2*) no significant regulations on the mRNA level were observed, while collagen protein was significantly increased.

This discrepancy between the WNT induced increase of total collagen protein amount and the unaffected mRNA levels of *Colla1* and *Colla2* could be referred to mRNA upregulation of other fibrillar collagen types than the analyzed ones. Furthermore, a significant change in collagen amount was observed after 20 h. During this time not necessarily directly WNT

induced pathways do have to lead to different protein patterns inside the fibroblasts. The discrepancy between mRNA and protein level suggests more complex ways of regulation including crosstalks to other profibrotic pathways or expression of still unknown target genes as intermediary effectors. Moreover, the large number of posttranslational modification of collagen before being secreted offers contact points for regulation mechanisms. These different explanation approaches should be included in further investigations, as well as a protein analysis that is able to distinguish between different collagen types.

Transcription of Fibronectin (*Fn*), another ECM component that is expressed in interstitial fibroblasts and recently has been assigned a causative role in pulmonary fibrosis¹⁰³ was not significantly regulated, proposing WNT/ β -catenin signaling not to be directly contributing to this part of the pathogenesis. In contrast, the main known myofibroblast activation marker α *Sma* exhibited significant upregulation after 6 h stimulation whereas fibroblast-specific protein (*Fsp*) 1¹⁰⁴ and Vimentin (*Vim*) were not regulated. This is in accordance with the assumption of WNT being causative for a phenotypic switch of inactive fibroblasts to activated myofibroblasts as α *Sma* is the most specific marker for this fibroblast phenotype.

To reveal possible crosstalks to pathways already known to be involved in IPF pathogenesis, effects on transcription of *Tgf- β 1*^{80,105} and arginase (*Arg*) 1 and 2^{81,106} were analyzed. TGF β -1 is known to induce collagen production in fibroblasts^{21,80} and a connection between WNT/ β -catenin pathway and TGF- β has already been reported¹⁰⁷. Additionally, by catalyzing L-arginine the arginases provide L-proline that is generated sequentially from L-ornithine and L-arginine and forms an important part of the procollagen polypeptide⁸¹. Our analysis did not reveal any regulation of either *Tgf- β -1* or *Arg* on the mRNA level, suggesting a different origin of collagen increase so far.

In their study about the functional role and species specific contribution of arginases in pulmonary fibrosis, Kitowska *et al.* (2008) also emphasize the importance of posttranslational processing for regulating mechanisms of collagen⁸¹. They showed that TGF β -1 induces *Arg 1* expression as well as a collagen increase on mRNA and protein level in mouse fibroblasts. Whereas *Arg* inhibition attenuated the TGF β -1 induced collagen increase on protein level, the inhibitory effect did not affect the mRNA level. This discrepancy between collagen mRNA and protein level stands in accordance to the observations in the present study.

After analysing the functional effects of WNT3a on fibroblasts, a similar investigation was performed with WNT1-inducible Signaling Protein 1 (WISP1) or CCN4. This member of the CCN family of secreted cysteine-rich regulatory proteins⁶⁵ was chosen for different reasons: WISP1 is encoded by a WNT/ β -catenin downstream target gene⁶⁹ and thus, an effector of

WNT/ β -catenin signaling that is involved in pulmonary fibrosis^{61,62}. Additionally, a role of CCN family members as signal transducers in developmental and pathologic processes is strongly suggested^{66,69-75}. In detail, not only the association to WNT signaling suggests a role of WISP1 in lung fibrosis, moreover the molecule itself has already been shown to be upregulated in IPF lung homogenates⁶³. In our laboratory, an increased expression of WISP1 in homogenates and alveolar epithelial cells type II (ATII) was observed in samples of experimental lung fibrosis and IPF. Localized next to hyperplastic ATII cells *in vivo* and *in vitro* the protein was shown to have autocrine proliferative effects on this cell type. Furthermore, WISP1 treatment resulted in an increase of profibrotic cytokines like *Mmp7*¹⁰⁸ in these cells. Together with the observation that lung fibrosis *in vivo* could be attenuated by inhibition of WISP1 these data suggest a key pathogenic role of this WNT target in initiation and perpetuation of IPF. Whereas ATII cells were the cell type that exhibited expression as well as autocrine affection by WISP1, in fibroblasts - the key effector cells of the disease - enhanced expression of the protein was not observed. In this context we considered fibroblasts as possible target cells of paracrine WISP1 binding⁶⁶. This suggestion was strengthened by the observation that CTGF, another member of the CCN family, has already been shown to stimulate fibroblast matrix production and myofibroblast differentiation in a paracrine fashion¹⁰⁹.

Finally, all these findings allowed the hypothesis that WISP1 contributes to IPF pathogenesis by having profibrotic effects on lung fibroblasts. Therefore, its functional effects were analyzed in the same way as before with WNT3a.

A recent publication by Colston et al.⁷³ demonstrated a proliferative effect of WISP1 on cardiac fibroblasts, which suggested a role of the protein in remodeling of myocardial infarction. In contrast to these observations, in the present study no influence on fibroblast proliferation was detected. Thus, not just cell type specific but also organ specific downstream effects of WISP1 can be proposed. These differences could possibly be explained by elucidating still unclear mechanisms of intracellular mechanisms after WISP binding to the cell surface considering variable environmental conditions of the cells in different tissues and organs.

To analyze activation of the fibroblasts and the possible influence of WISP1 on ECM deposition, localization, and amount of collagen in the cells were determined. Immunofluorescence staining of collagen inside the cytoplasm of all cells and also slightly beyond indicated general ability of the fibroblasts to produce and secrete collagen, but did not allow determining quantitative differences between stimulated and unstimulated fibroblasts.

In regard to quantitative measurement of collagen content by Sircol Collagen Assay, demonstrated results align with the effects described by Colston et al. (2007)⁷³. Though, they observed a significant collagen increase of cardiac fibroblasts after 72 h, whereas in the current study the increase was already discovered after 20 h of stimulation with WISP1.

The relevance of these possibly profibrotic effects can be emphasized as the increase of collagen production of subconfluent fibroblasts was even higher than after treatment with TGF- β 1, similar to the results of the stimulation experiments with WNT3a.

In contrast to the results for WNT3a, enhanced collagen synthesis after WISP1 treatment of the fibroblasts can be explained by preceding activation of the cells and transcriptional upregulation of fibrillar collagens. This can be stated because of increased expression of type I collagen α 1 (*Colla1*) and type I collagen α 2 (*Colla2*) mRNA after 12 h stimulation with WISP1. Whereas other collagen types IV (*Col4*) and VII (*Col7*) did not reveal relevant upregulation, the expression of the ECM component Fibronectin (*Fn*) 1 was increased after 6 h, underlining the capacity of WISP1 to trigger the enhancement of ECM deposition.

A contribution of WISP1 to the phenotype switch of inactivated fibroblasts to myofibroblasts and thereby activation of the cells can be assumed because of transcriptional upregulation of the (myo)-fibroblast activation marker α *Sma* and fibroblast-specific protein 1 (*Fsp1*), which was already reported to play a role in epithelial-to-mesenchymal transition (EMT) in tissue fibrosis¹⁰⁴.

Disturbed ECM degradation belongs to pulmonary fibrosis as well as excessive production. To reveal possible effects of WISP1 in this subarea, further research projects are necessary. However, to touch on this subject, transcriptional regulation of a potentially involved molecule was checked: Plasminogen activator inhibitor (PAI) 1 belongs to the plasmin system, which plays a crucial role for ECM degradation. By inhibiting plasminogen activators, PAI-1 is able to regulate the activation from plasminogen to plasmin. Thereby it has the capacity to inhibit plasmin induced ECM degradation or activation of degrading molecules respectively⁸². Expression of PAI-1 is known to be elevated in experimental fibrosis models and pulmonary fibrosis⁸². Transcriptional regulation via WISP1 in fibroblasts could have delivered information about the involvement of the ligand in ECM degradation. Increase of *Pai-1* after stimulation would have argued for profibrotic features of WISP1. However, no significant upregulation has been observed for the investigated time points.

Summarizing the presented data a profibrotic role of WISP1 on lung fibroblasts can be stated. Increased expression of (myo-) fibroblast activation markers argues for this conclusion as well as enhanced collagen production on protein level with according upregulation of type I

collagen on mRNA level. These observations predominantly have to be considered as paracrine effects of WISP1 on fibroblasts in IPF as its expression was exclusively enhanced in alveolar epithelial cells⁷⁷. An autocrine role of the ligand in IPF fibroblasts is rather unlikely because in our laboratory we neither detected increased mRNA nor protein expression of WISP1 in fibroblasts from experimental lung fibrosis and IPF lungs⁷⁷. Therefore, the explanation approach that WISP1 is encoded by a WNT responsive gene and thus, could have been an intermediary effector for profibrotic WNT effects, takes a back seat. In fact, data from the present study suggest WISP1 as a paracrine profibrotic ligand on lung fibroblasts as a result from enhanced expression and secretion by hyperplastic ATII cells within the progression of IPF.

5.3. Conclusions and future perspectives in regard to IPF pathogenesis

Idiopathic pulmonary fibrosis (IPF) still has the worst prognosis of all idiopathic interstitial pneumonias (IIP). Appropriate therapies do not exist yet, which is mostly due to the fact that the pathomechanisms of the disease are not completely understood. However, extensive research in this issue has revealed WNT/ β -catenin signaling including the WNT-target molecule WISP1 to be involved in processes leading to progression of fibrosis³⁶.

Experiments of this study were performed in order to test the hypothesis that WNT/ β -catenin signaling can be activated in lung fibroblasts by paracrine binding of WNT ligands and that WNT3a and the WNT target molecule WISP1 have profibrotic effects on lung fibroblasts, thereby contributing to the impaired crosstalk between ATII cells and fibroblasts during the pathogenesis of IPF. Data are received from *in vitro* experiments with NIH-3T3 mouse fibroblasts. To evaluate the relevance of the obtained results in regard to IPF pathogenesis further experiments with primary and human cells as well as *in vivo* experiments are desirable and necessary. Nevertheless, the used fibroblast cell line is well established in culture and frequently used for basic research indicating reactions of the human system.

Concerning the question, if WNT/ β -catenin signaling can be activated in fibroblasts, it was demonstrated that pathway components are expressed constitutively in these cells and target genes after stimulation with WNT3a. These observations confirmed that fibroblasts exhibit WNT responsiveness. Functional relevance thereof was demonstrated by pointing out paracrine effects of WNT3a particularly with regard to a possible profibrotic role. Whereas proliferation remained unaffected, a collagen increase on protein level indicated influence of

WNT in a profibrotic manner. Furthermore, a contribution of activated WNT/ β -catenin signaling to the phenotype switch of inactivated fibroblasts to activated myofibroblasts can be assumed because of transcriptional upregulation of a fibroblast activation marker. The collagen increase on protein level could not be clearly ascribed to upregulation on mRNA level. As this discrepancy could not be explained by analysis of potential crosstalk partners or molecules possibly involved in posttranslational modification changes, further experiments are required to enlighten reasons for the unambiguous collagen increase inside the cells after activation of the β -catenin pathway by binding of WNT3a to the cell surface.

The glycoprotein WISP1, encoded by a WNT target gene, was also analyzed as a paracrine ligand with potential profibrotic effects on fibroblasts. Experimental results demonstrate that WISP1 leads to fibroblast activation as well as enhanced ECM deposition. Here, a causative connection between collagen increase on protein level and upregulation of corresponding mRNA can be stated.

Analysing fibroblast activation markers and collagen production in fibroblasts was mainly aimed at elucidating possible effects of WNT3a or WISP1 on one of the key pathogenic mechanisms that characterize the fatal course of IPF: extensive ECM deposition by activated fibroblasts. However, ECM imbalance during fibrosis not only consists of extensive ECM accumulation but also disturbed degradation. Thus, another interesting research focus would be to check expression, synthesis and secretion of molecules that are involved into ECM degradation like matrixmetalloproteinases (MMP) or tissue inhibitors of metalloproteinases (TIMP)⁸⁰. These molecules could be influenced during IPF as well as mediators of apoptosis⁷². As this part was not the focus of the current study, on transcriptional and protein level further investigation is possible and required to reveal the functional effects of both ligands entirely.

From the results of the present study can be concluded that WNT3a and WISP1 act in a paracrine fashion as profibrotic mediators on fibroblasts *in vitro*. Together with current research results about IPF and WNT signaling this detection strongly suggests WNT/ β -catenin signaling and its effectors to be functional in fibroblasts during the pathogenesis of IPF. Inhibiting WNT/ β -catenin signal transduction or antagonizing its downstream effectors could possibly prevent fibroblasts from advancing the diseases' progression. Thus, elucidating the downstream mechanisms and the effects of WNT and WISP on fibroblasts *in vivo* and in the human system is a worthwhile aim for further investigation.

6. Appendix

6.1 Primer sequences and amplicon sizes

Gene	Accession		Sequences (5' → 3')	Length	Amplicon
<i>Arg1</i>	NM007482	for	gga acc cag aga gag cat ga	20bp	132bp
		rev	ttt ttc cag cag acc agc tt	20bp	
<i>Arg2</i>	NM009705	for	acc agg aac tgg ctg aag tg	20bp	141bp
		rev	tga gca tca acc cag atg ac	20bp	
β - <i>Cat</i>	NM007614	for	tca aga gag caa gct cat cat tct	24bp	115bp
		rev	cac ctt cag cac tct tgt g	22bp	
<i>Colla1</i>	NM007742	for	cca aga aga cat ccc tga agt ca	23bp	128bp
		rev	tgc acg tca tgc cac aca	18bp	
<i>Colla2</i>	NM007743	for	agc ttt gtg gat acg cgg act	21bp	86bp
		rev	tcg tac tga tcc cga ttg ca	20bp	
<i>Ctgf</i>	NM010217	for	ctt ctg cga ttt cgg ctc c	19p	115bp
		rev	tgc ttt gga agg act cac cg	20bp	
<i>CycD1</i>	NM007631	for	atg cca gag gcg gat gag a	19bp	98bp
		rev	atg gag ggt ggg ttg gaa at	20bp	
<i>Fn</i>	NM010233	for	gtg tag cac aac ttc caa tta cga a	25bp	90bp
		rev	gga att tcc gcc tgc agt ct	20bp	
<i>Fsp1</i>	NM011311	for	agg agc tac tga cca ggg agc t	22bp	102bp
		rev	tca ttg tcc ctg ttg ctg tcc	21bp	

Gene	Accession		Sequences (5' → 3')	Length	Amplicon
<i>Fzd1</i>	NM021457	for	aaa cag cac agg ttc tgc aaa a	22bp	58bp
		rev	tgg gcc ctc tcg ttc ctt	18bp	
<i>Fzd2</i>	NM020510	for	tcc atc tgg tgg gtg att ctg	21bp	66bp
		rev	ctc gtg gcc cca ctt cat t	19bp	
<i>Fzd3</i>	NM021458	for	gcc tat agc gag tgt tca aaa ctc a	25bp	78bp
		rev	tgg aaa cct act gca ctc cat atc t	25bp	
<i>Fzd4</i>	NM008055	for	gcc cca gaa cga cca caa	18bp	64bp
		rev	ggg caa ggg aac ctc ttc at	20bp	
<i>Fzd5</i>	NM02272	for	ccc acc gca cgt ttt cc	17bp	63bp
		rev	gct ttt cat ttc gct tgt tat c	25bp	
<i>Fzd6</i>	NM008056	for	gtt cta ccc tgt cgg aaa ttg tg	23bp	146bp
		rev	gtg gat gag aag tta cag gaa cag tgt	27bp	
<i>Fzd7</i>	NM008057	for	gcc agg tgg atg gtg acc ta	20bp	68bp
		rev	ccg caa tgc atc cac act ag	20bp	
<i>Fzd8</i>	NM008058	for	gca agg agg ccc aac taa gac	21bp	58bp
		rev	gag gcc caa gcg gat ca	17bp	
<i>Gsk3β</i>	NM019827	for	ttt gag ctg gta ccc tag gat ga	23bp	75bp
		rev	ttc ttc gct ttc cga tgc a	19bp	
<i>Lef1</i>	NM010703	for	ggc ggc gtt gga cag at	17bp	67bp
		rev	cac ccg tga tgg gat aaa cag	21bp	

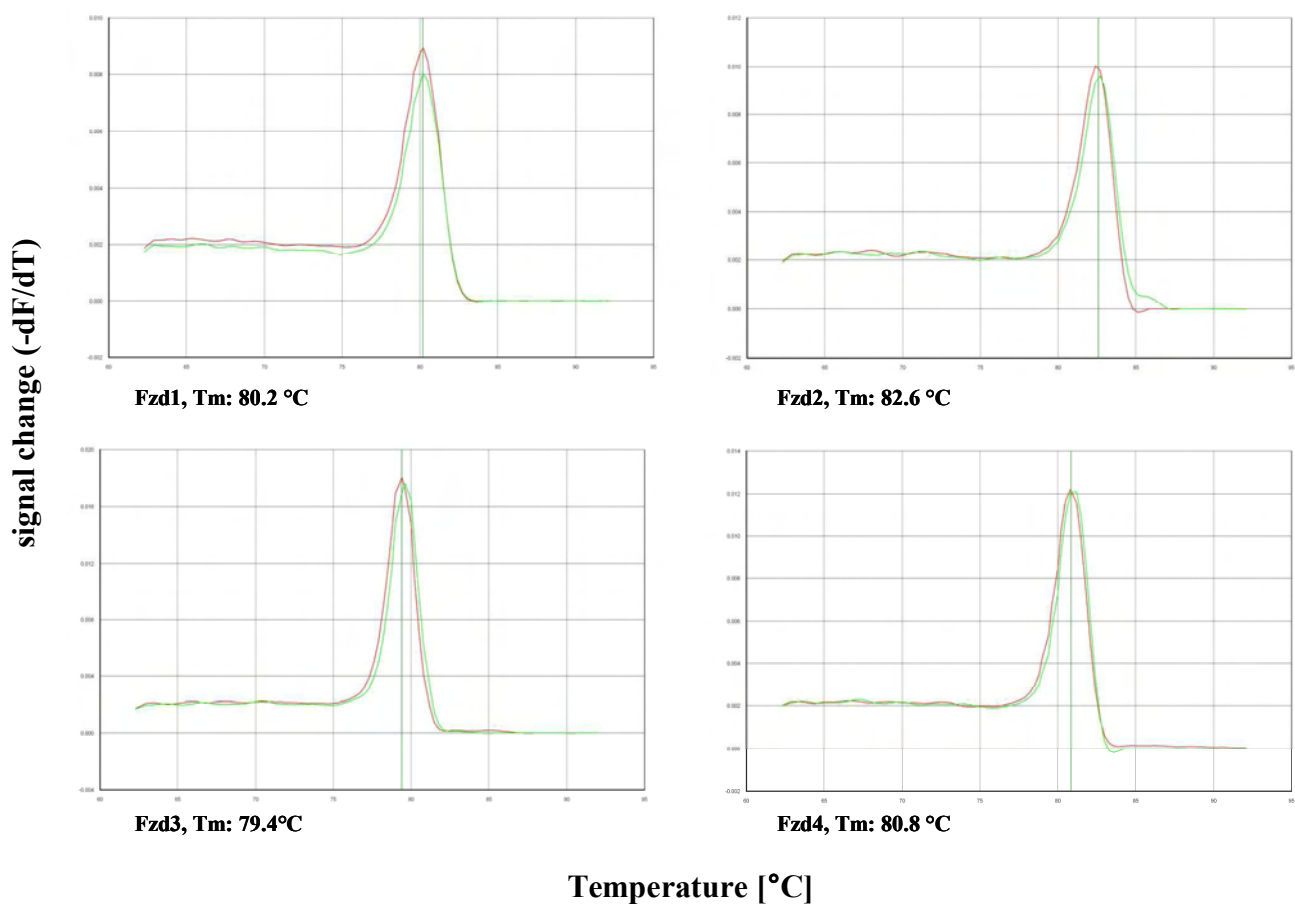
Gene	Accession		Sequences (5' → 3')	Length	Amplicon
<i>LRP5</i>	NM008513	for	caa cgt gga cgt gtt tta ttc ttc	24 bp	138 bp
		rev	cag cga ctg gtg ctg tag tca	21 bp	
<i>LRP6</i>	NM008514	for	cca ttc ctc tca ctg gtg tca a	22 bp	146 bp
		rev	gcc aaa ctc tac cac atg ttc ca	23 bp	
<i>Pai1</i>	NM008871	for	gtc ttt ccg acc aag agc ag	20 bp	104 bp
		rev	gac aaa ggc tgt gga gga ag	20 bp	
<i>Pbgd</i>	NM135511	for	atg tcc ggt aac ggc ggc	18 bp	121 bp
		rev	ggt aca agg ctt tca cga	22 bp	
<i>αSma</i>	NM007392	for	gct ggt gat gat gct ccc a	19 bp	80 bp
		rev	gcc cat tcc aac cat tac tcc	21 bp	
<i>Tgfβ-1</i>	NM011577	for	agg tca ccc gcg tgc taa t	19 bp	115 bp
		rev	ggc act get tcc cga atg t	19 bp	
<i>Wnt1</i>	NM021279	for	caa atg gca att ccg aaa cc	20 bp	111 bp
		rev	gat tgc gaa gat gaa cgc tg	20 bp	
<i>Wnt3a</i>	NM009522	for	gca cca ccg tga gca aca	18 bp	56 bp
		rev	ggg tgg ctt tgt cca gaa ca	20 bp	
<i>Wnt8b</i>	NM011720	for	tgg gac cgt tgg aat tgc	18 bp	72 bp
		rev	ccg gtt agc gct tcg aag t	19 bp	
<i>W10a</i>	NM009518	for	atg agt gcc agc atc agt tcc	21 bp	123 bp
		rev	gcg tag gcg aaa gca ctc tc	20 bp	

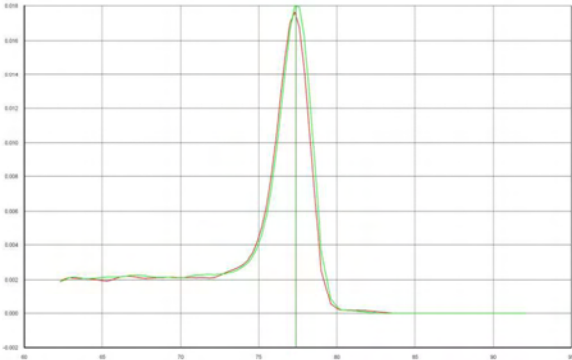
Gene	Accession		Sequences (5' → 3')	Length	Amplicon
<i>Wnt10b</i>	NM011718	for	tgg gac gcc agg tgg taa	18 bp	60 bp
		rev	ctg acg ttc cat ggc att tg	20 bp	
<i>Wnt11</i>	NM009519	for	ccc cca act acc tgc ttg ac	20 bp	68 bp
		rev	ggc cga cag ggc ata cac	18 bp	

Table 3. Primer sequences and amplicon sizes.

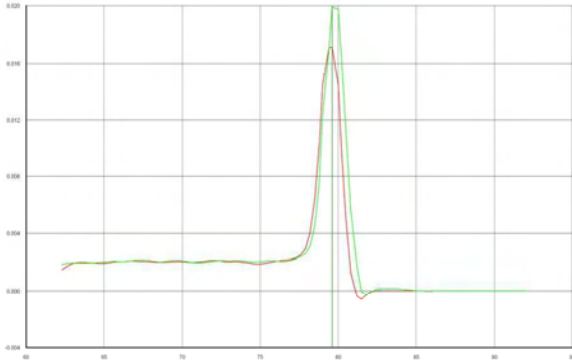
The primer sets work under identical real-time PCR cycling conditions with similar efficiencies to obtain simultaneous amplification in the same run. Sequences were taken from GeneBank, Accession numbers are given.

6.2 Dissociation curves

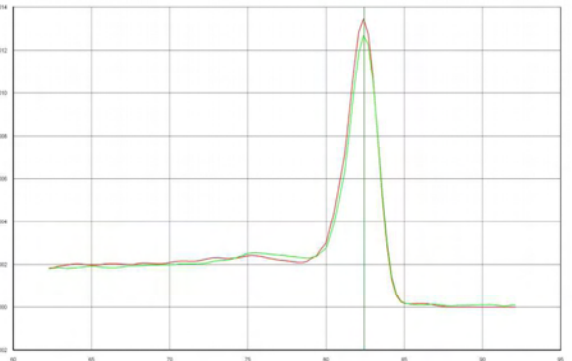




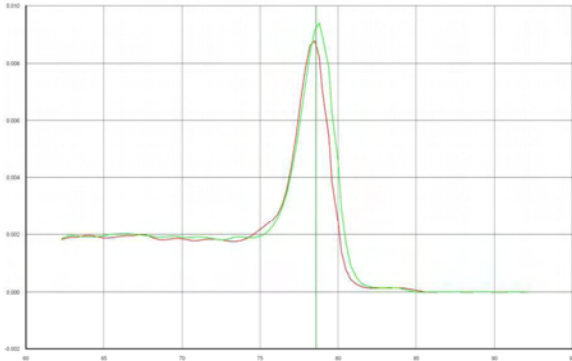
Fzd5, Tm: 77.4 °C



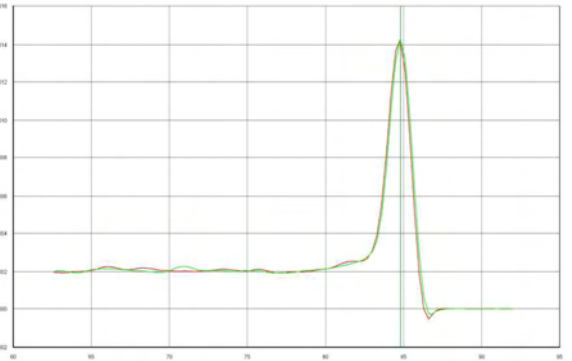
Fzd6, Tm: 79.6 °C



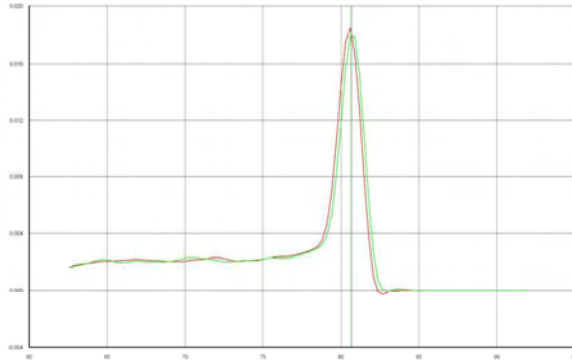
Fzd7, Tm: 82.4 °C



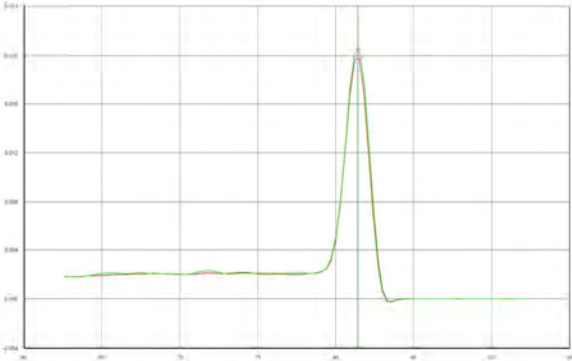
Fzd8, Tm: 78.6 °C



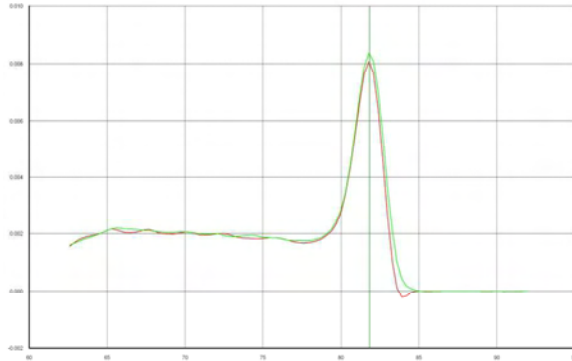
LRP5, Tm: 84.8 °C



LRP6, Tm: 80.7 °C



β-Cat, Tm: 81.4 °C



GSK3β, Tm: 81.8 °C

Temperature [°C]

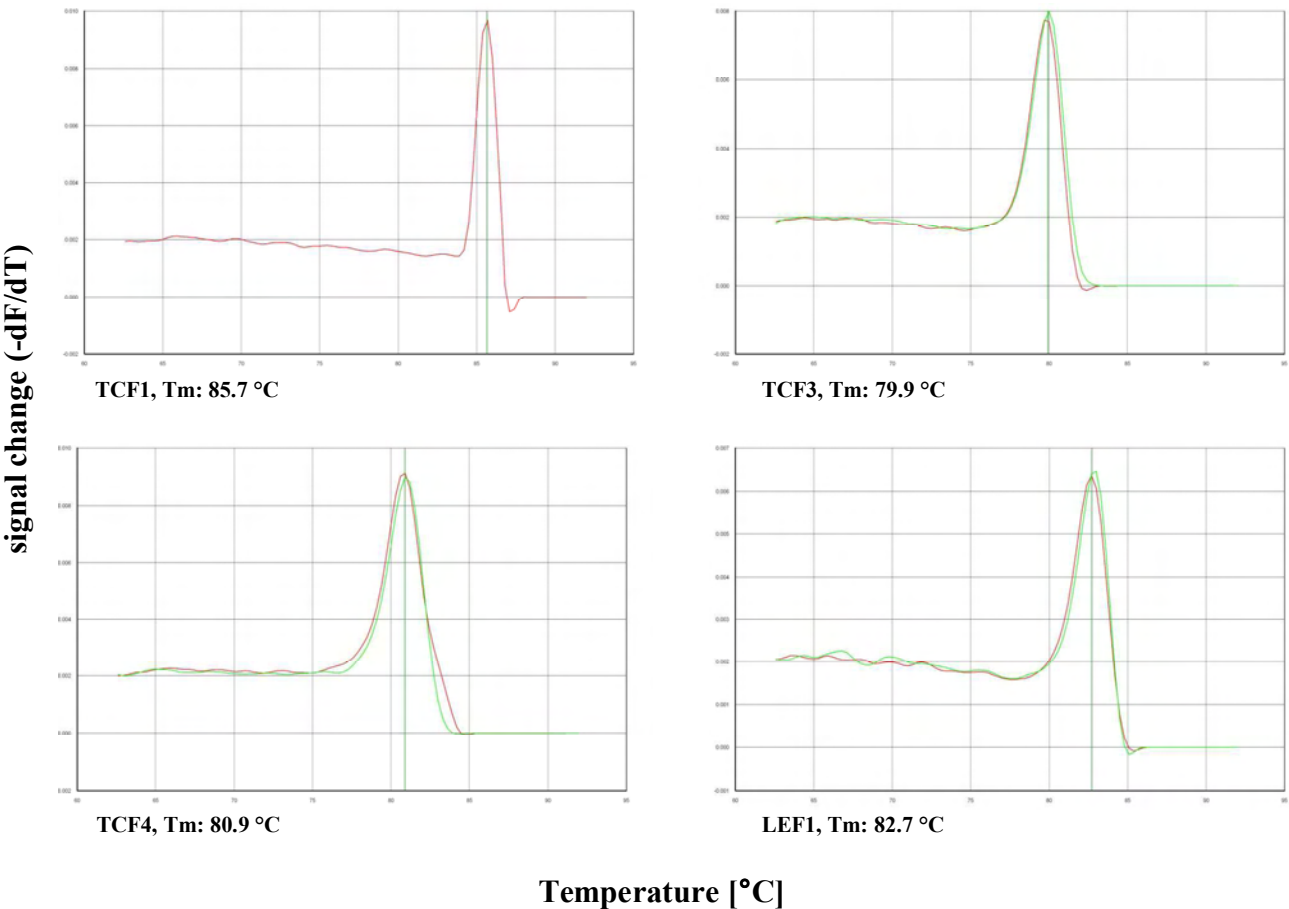


Figure 14. Dissociation curves
Primer sets of WNT/ β -catenin pathway components

7. References

1. American Thoracic Society/European Respiratory Society International Multidisciplinary Consensus Classification of the Idiopathic Interstitial Pneumonias. This joint statement of the American Thoracic Society (ATS), and the European Respiratory Society (ERS) was adopted by the ATS board of directors, June 2001 and by the ERS Executive Committee, June 2001. *Am J Respir Crit Care Med* **165**, 277-304 (2002).
2. Chapman, H.A. Disorders of lung matrix remodeling. *J Clin Invest* **113**, 148-157 (2004).
3. Martinez, F.J., *et al.* The clinical course of patients with idiopathic pulmonary fibrosis. *Ann Intern Med* **142**, 963-967 (2005).
4. Visscher, D.W. & Myers, J.L. Histologic spectrum of idiopathic interstitial pneumonias. *Proceedings of the American Thoracic Society* **3**, 322-329 (2006).
5. Pardo, A. & Selman, M. Idiopathic pulmonary fibrosis: new insights in its pathogenesis. *The international journal of biochemistry & cell biology* **34**, 1534-1538 (2002).
6. Dempsey, O.J. Clinical review: idiopathic pulmonary fibrosis--past, present and future. *Respiratory medicine* **100**, 1871-1885 (2006).
7. Selman, M., King, T.E. & Pardo, A. Idiopathic pulmonary fibrosis: prevailing and evolving hypotheses about its pathogenesis and implications for therapy. *Ann Intern Med* **134**, 136-151 (2001).
8. Thannickal, V.J., Toews, G.B., White, E.S., Lynch, J.P., 3rd & Martinez, F.J. Mechanisms of pulmonary fibrosis. *Annu Rev Med* **55**, 395-417 (2004).
9. Walter, N., Collard, H.R. & King, T.E., Jr. Current perspectives on the treatment of idiopathic pulmonary fibrosis. *Proceedings of the American Thoracic Society* **3**, 330-338 (2006).
10. Gross, T.J. & Hunninghake, G.W. Idiopathic pulmonary fibrosis. *The New England journal of medicine* **345**, 517-525 (2001).
11. Gunther, A., Markart, P., Eickelberg, O. & Seeger, W. [Pulmonary Fibrosis-a Therapeutic Dilemma?]. *Med Klin (Munich)* **101**, 308-312 (2006).
12. Selman, M. & Pardo, A. Idiopathic pulmonary fibrosis: an epithelial/fibroblastic cross-talk disorder. *Respir Res* **3**, 3 (2002).
13. Katzenstein, A.L. & Myers, J.L. Idiopathic pulmonary fibrosis: clinical relevance of pathologic classification. *Am J Respir Crit Care Med* **157**, 1301-1315 (1998).
14. Flaherty, K.B., *et al.* Prognostic Value of Fibroblastic Foci in Patients With Usual Interstitial Pneumonia. *CHEST* **120**, 76-77 (2001).
15. King, T.E., Jr., *et al.* Idiopathic pulmonary fibrosis: relationship between histopathologic features and mortality. *Am J Respir Crit Care Med* **164**, 1025-1032 (2001).
16. Nicholson, A.G., *et al.* The relationship between individual histologic features and disease progression in idiopathic pulmonary fibrosis. *Am J Respir Crit Care Med* **166**, 173-177 (2002).
17. Grundmann, E. Lungenfibrose. *Spezielle Pathologie. Farbatlas der makroskopischen und mikroskopischen Pathologie*, 58, E21 (1994).

18. Strieter, R.M. Pathogenesis and natural history of usual interstitial pneumonia: the whole story or the last chapter of a long novel. *Chest* **128**, 526S-532S (2005).
19. Gauldie, J., Kolb, M. & Sime, P.J. A new direction in the pathogenesis of idiopathic pulmonary fibrosis? *Respir Res* **3**, 1 (2002).
20. Eickelberg, O., *et al.* Transforming growth factor-beta1 induces interleukin-6 expression via activating protein-1 consisting of JunD homodimers in primary human lung fibroblasts. *J Biol Chem* **274**, 12933-12938 (1999).
21. Ignatz, R.A. & Massague, J. Transforming growth factor-beta stimulates the expression of fibronectin and collagen and their incorporation into the extracellular matrix. *J Biol Chem* **261**, 4337-4345 (1986).
22. Lorena, D., Uchio, K., Costa, A.M. & Desmouliere, A. Normal scarring: importance of myofibroblasts. *Wound Repair Regen* **10**, 86-92 (2002).
23. Thannickal, V.J., Aldweib, K.D., Rajan, T. & Fanburg, B.L. Upregulated expression of fibroblast growth factor (FGF) receptors by transforming growth factor-beta1 (TGF-beta1) mediates enhanced mitogenic responses to FGFs in cultured human lung fibroblasts. *Biochem Biophys Res Commun* **251**, 437-441 (1998).
24. Uhal, B.D., *et al.* Alveolar epithelial cell death adjacent to underlying myofibroblasts in advanced fibrotic human lung. *Am J Physiol* **275**, L1192-1199 (1998).
25. Kuhn, C. & McDonald, J.A. The roles of the myofibroblast in idiopathic pulmonary fibrosis. Ultrastructural and immunohistochemical features of sites of active extracellular matrix synthesis. *Am J Pathol* **138**, 1257-1265 (1991).
26. Scotton, C.J. & Chambers, R.C. Molecular targets in pulmonary fibrosis: the myofibroblast in focus. *Chest* **132**, 1311-1321 (2007).
27. Zhang, K., Rekhter, M.D., Gordon, D. & Phan, S.H. Myofibroblasts and their role in lung collagen gene expression during pulmonary fibrosis. A combined immunohistochemical and in situ hybridization study. *Am J Pathol* **145**, 114-125 (1994).
28. Kelly, M., Kolb, M., Bonniaud, P. & Gauldie, J. Re-evaluation of fibrogenic cytokines in lung fibrosis. *Curr Pharm Des* **9**, 39-49 (2003).
29. Nusse, R. & Varmus, H.E. Many tumors induced by the mouse mammary tumor virus contain a provirus integrated in the same region of the host genome. *Cell* **31**, 99-109 (1982).
30. Rijsewijk, F., *et al.* The Drosophila homolog of the mouse mammary oncogene int-1 is identical to the segment polarity gene wingless. *Cell* **50**, 649-657 (1987).
31. Moon, R.T., Kohn, A.D., De Ferrari, G.V. & Kaykas, A. WNT and beta-catenin signalling: diseases and therapies. *Nat Rev Genet* **5**, 691-701 (2004).
32. Nusse, R. Wnt signaling in disease and in development. *Cell Res* **15**, 28-32 (2005).
33. Mikels, A.J. & Nusse, R. Wnts as ligands: processing, secretion and reception. *Oncogene* **25**, 7461-7468 (2006).
34. Komekado, H., Yamamoto, H., Chiba, T. & Kikuchi, A. Glycosylation and palmitoylation of Wnt-3a are coupled to produce an active form of Wnt-3a. *Genes Cells* **12**, 521-534 (2007).
35. Logan, C.Y. & Nusse, R. The Wnt signaling pathway in development and disease. *Annu Rev Cell Dev Biol* **20**, 781-810 (2004).

36. Königshoff, M. & Eickelberg, O. WNT Signaling in Lung Disease: A Failure or a Regeneration Signal? *American journal of respiratory cell and molecular biology* (2009).
37. Mlodzik, M. Planar cell polarization: do the same mechanisms regulate Drosophila tissue polarity and vertebrate gastrulation? *Trends Genet* **18**, 564-571 (2002).
38. Gordon, M.D. & Nusse, R. Wnt signaling: multiple pathways, multiple receptors, and multiple transcription factors. *J Biol Chem* **281**, 22429-22433 (2006).
39. Bhanot, P., *et al.* A new member of the frizzled family from Drosophila functions as a Wingless receptor. *Nature* **382**, 225-230 (1996).
40. Tamai, K., *et al.* LDL-receptor-related proteins in Wnt signal transduction. *Nature* **407**, 530-535 (2000).
41. Tolwinski, N.S. & Wieschaus, E. Rethinking WNT signaling. *Trends Genet* **20**, 177-181 (2004).
42. Daniels, D.L. & Weis, W.I. Beta-catenin directly displaces Groucho/TLE repressors from Tcf/Lef in Wnt-mediated transcription activation. *Nature structural & molecular biology* **12**, 364-371 (2005).
43. He, T.C., *et al.* Identification of c-MYC as a target of the APC pathway. *Science* **281**, 1509-1512 (1998).
44. Shtutman, M., *et al.* The cyclin D1 gene is a target of the beta-catenin/LEF-1 pathway. *Proc Natl Acad Sci U S A* **96**, 5522-5527 (1999).
45. Tetsu, O. & McCormick, F. Beta-catenin regulates expression of cyclin D1 in colon carcinoma cells. *Nature* **398**, 422-426 (1999).
46. Crawford, H.C., *et al.* The metalloproteinase matrilysin is a target of beta-catenin transactivation in intestinal tumors. *Oncogene* **18**, 2883-2891 (1999).
47. Kikuchi, A. Tumor formation by genetic mutations in the components of the Wnt signaling pathway. *Cancer science* **94**, 225-229 (2003).
48. Satoh, S., *et al.* AXIN1 mutations in hepatocellular carcinomas, and growth suppression in cancer cells by virus-mediated transfer of AXIN1. *Nat Genet* **24**, 245-250 (2000).
49. Lammi, L., *et al.* Mutations in AXIN2 cause familial tooth agenesis and predispose to colorectal cancer. *Am J Hum Genet* **74**, 1043-1050 (2004).
50. Johnson, M.L. & Rajamannan, N. Diseases of Wnt signaling. *Reviews in endocrine & metabolic disorders* **7**, 41-49 (2006).
51. Huang, C.L., *et al.* Wnt1 overexpression promotes tumour progression in non-small cell lung cancer. *Eur J Cancer* **44**, 2680-2688 (2008).
52. Nakashima, T., *et al.* Wnt1 overexpression associated with tumor proliferation and a poor prognosis in non-small cell lung cancer patients. *Oncology reports* **19**, 203-209 (2008).
53. Kim, J., *et al.* Wnt inhibitory factor inhibits lung cancer cell growth. *The Journal of thoracic and cardiovascular surgery* **133**, 733-737 (2007).
54. Cheon, S.S., *et al.* beta-Catenin stabilization dysregulates mesenchymal cell proliferation, motility, and invasiveness and causes aggressive fibromatosis and hyperplastic cutaneous wounds. *Proc Natl Acad Sci U S A* **99**, 6973-6978 (2002).

55. Cheon, S.S., Nadesan, P., Poon, R. & Alman, B.A. Growth factors regulate beta-catenin-mediated TCF-dependent transcriptional activation in fibroblasts during the proliferative phase of wound healing. *Exp Cell Res* **293**, 267-274 (2004).
56. Cheng, J.H., *et al.* Wnt antagonism inhibits hepatic stellate cell activation and liver fibrosis. *Am J Physiol Gastrointest Liver Physiol* **294**, G39-49 (2008).
57. Surendran, K., McCaul, S.P. & Simon, T.C. A role for Wnt-4 in renal fibrosis. *Am J Physiol Renal Physiol* **282**, F431-441 (2002).
58. Surendran, K., Schiavi, S. & Hruska, K.A. Wnt-dependent beta-catenin signaling is activated after unilateral ureteral obstruction, and recombinant secreted frizzled-related protein 4 alters the progression of renal fibrosis. *J Am Soc Nephrol* **16**, 2373-2384 (2005).
59. Morrisey, E.E. Wnt signaling and pulmonary fibrosis. *Am J Pathol* **162**, 1393-1397 (2003).
60. Mucenski, M.L., *et al.* beta-Catenin is required for specification of proximal/distal cell fate during lung morphogenesis. *J Biol Chem* **278**, 40231-40238 (2003).
61. Chilosi, M., *et al.* Aberrant Wnt/beta-catenin pathway activation in idiopathic pulmonary fibrosis. *Am J Pathol* **162**, 1495-1502 (2003).
62. Königshoff, M., *et al.* Functional Wnt signaling is increased in idiopathic pulmonary fibrosis. *PLoS ONE* **3**, e2142 (2008).
63. Selman, M., *et al.* Gene expression profiles distinguish idiopathic pulmonary fibrosis from hypersensitivity pneumonitis. *Am J Respir Crit Care Med* **173**, 188-198 (2006).
64. Lewis, C.C., *et al.* Disease-specific gene expression profiling in multiple models of lung disease. *Am J Respir Crit Care Med* **177**, 376-387 (2008).
65. Perbal, B. CCN proteins: multifunctional signalling regulators. *Lancet* **363**, 62-64 (2004).
66. Brigstock, D.R. The CCN family: a new stimulus package. *J Endocrinol* **178**, 169-175 (2003).
67. Planque, N. & Perbal, B. A structural approach to the role of CCN (CYR61/CTGF/NOV) proteins in tumourigenesis. *Cancer cell international* **3**, 15 (2003).
68. Lau, L.F. & Lam, S.C. The CCN family of angiogenic regulators: the integrin connection. *Exp Cell Res* **248**, 44-57 (1999).
69. Pennica, D., *et al.* WISP genes are members of the connective tissue growth factor family that are up-regulated in wnt-1-transformed cells and aberrantly expressed in human colon tumors. *Proc Natl Acad Sci U S A* **95**, 14717-14722 (1998).
70. Xu, L., Corcoran, R.B., Welsh, J.W., Pennica, D. & Levine, A.J. WISP-1 is a Wnt-1- and beta-catenin-responsive oncogene. *Genes Dev* **14**, 585-595 (2000).
71. You, Z., *et al.* Wnt signaling promotes oncogenic transformation by inhibiting c-Myc-induced apoptosis. *J Cell Biol* **157**, 429-440 (2002).
72. Su, F., Overholtzer, M., Besser, D. & Levine, A.J. WISP-1 attenuates p53-mediated apoptosis in response to DNA damage through activation of the Akt kinase. *Genes Dev* **16**, 46-57 (2002).
73. Colston, J.T., *et al.* Wnt-induced secreted protein-1 is a prohypertrophic and profibrotic growth factor. *American journal of physiology* **293**, H1839-1846 (2007).

74. Yu, C., Le, A.T., Yeger, H., Perbal, B. & Alman, B.A. NOV (CCN3) regulation in the growth plate and CCN family member expression in cartilage neoplasia. *J Pathol* **201**, 609-615 (2003).
75. Saxena, N., Banerjee, S., Sengupta, K., Zoubine, M.N. & Banerjee, S.K. Differential expression of WISP-1 and WISP-2 genes in normal and transformed human breast cell lines. *Mol Cell Biochem* **228**, 99-104 (2001).
76. Chen, P.P., *et al.* Expression of Cyr61, CTGF, and WISP-1 correlates with clinical features of lung cancer. *PLoS ONE* **2**, e534 (2007).
77. Königshoff, M., *et al.* WNT1-inducible signaling protein-1 mediates pulmonary fibrosis in mice and is upregulated in humans with idiopathic pulmonary fibrosis. *J Clin Invest* **119**, 772-787 (2009).
78. Wilhelm, J. & Pingoud, A. Real-time polymerase chain reaction. *Chembiochem* **4**, 1120-1128 (2003).
79. Hochberg, Y. & Benjamini, Y. More powerful procedures for multiple significance testing. *Statistics in medicine* **9**, 811-818 (1990).
80. Eickelberg, O., *et al.* Extracellular matrix deposition by primary human lung fibroblasts in response to TGF-beta1 and TGF-beta3. *Am J Physiol* **276**, L814-824 (1999).
81. Kitowska, K., *et al.* Functional role and species-specific contribution of arginases in pulmonary fibrosis. *Am J Physiol Lung Cell Mol Physiol* **294**, L34-45 (2008).
82. Liu, R.M. Oxidative stress, plasminogen activator inhibitor 1, and lung fibrosis. *Antioxidants & redox signaling* **10**, 303-319 (2008).
83. Lama, V.N. & Phan, S.H. The extrapulmonary origin of fibroblasts: stem/progenitor cells and beyond. *Proceedings of the American Thoracic Society* **3**, 373-376 (2006).
84. Hashimoto, N., Jin, H., Liu, T., Chensue, S.W. & Phan, S.H. Bone marrow-derived progenitor cells in pulmonary fibrosis. *J Clin Invest* **113**, 243-252 (2004).
85. Moore, B.B., *et al.* The Role of CCL12 in the Recruitment of Fibrocytes and Lung Fibrosis. *American journal of respiratory cell and molecular biology* (2006).
86. Phillips, R.J., *et al.* Circulating fibrocytes traffic to the lungs in response to CXCL12 and mediate fibrosis. *J Clin Invest* **114**, 438-446 (2004).
87. Kim, D.S., Collard, H.R. & King, T.E., Jr. Classification and natural history of the idiopathic interstitial pneumonias. *Proceedings of the American Thoracic Society* **3**, 285-292 (2006).
88. Willis, B.C., *et al.* Induction of epithelial-mesenchymal transition in alveolar epithelial cells by transforming growth factor-beta1: potential role in idiopathic pulmonary fibrosis. *Am J Pathol* **166**, 1321-1332 (2005).
89. Willis, B.C., Dubois, R.M. & Borok, Z. Epithelial Origin of Myofibroblasts during Fibrosis in the Lung. *Proceedings of the American Thoracic Society* **3**, 377-382 (2006).
90. Phan, S.H. The myofibroblast in pulmonary fibrosis. *Chest* **122**, 286S-289S (2002).
91. He, B. & Jablons, D.M. Wnt signaling in stem cells and lung cancer. *Ernst Schering Foundation symposium proceedings*, 27-58 (2006).

92. Klapholz-Brown, Z., Walmsley, G.G., Nusse, Y.M., Nusse, R. & Brown, P.O. Transcriptional program induced by wnt protein in human fibroblasts suggests mechanisms for cell cooperativity in defining tissue microenvironments. *PLoS ONE* **2**, e945 (2007).
93. Bilic, J., *et al.* Wnt induces LRP6 signalosomes and promotes dishevelled-dependent LRP6 phosphorylation. *Science* **316**, 1619-1622 (2007).
94. Forde, J.E. & Dale, T.C. Glycogen synthase kinase 3: a key regulator of cellular fate. *Cell Mol Life Sci* **64**, 1930-1944 (2007).
95. Alt, J.R., Cleveland, J.L., Hannink, M. & Diehl, J.A. Phosphorylation-dependent regulation of cyclin D1 nuclear export and cyclin D1-dependent cellular transformation. *Genes Dev* **14**, 3102-3114 (2000).
96. Raghu, G., Chen, Y.Y., Rusch, V. & Rabinovitch, P.S. Differential proliferation of fibroblasts cultured from normal and fibrotic human lungs. *Am Rev Respir Dis* **138**, 703-708 (1988).
97. Vuga, L.J., *et al.* WNT5A is a Regulator of Fibroblast Proliferation and Resistance to Apoptosis. *American journal of respiratory cell and molecular biology* (2009).
98. Hetzel, M., Bachem, M., Anders, D., Trischler, G. & Faehling, M. Different effects of growth factors on proliferation and matrix production of normal and fibrotic human lung fibroblasts. *Lung* **183**, 225-237 (2005).
99. Canty, E.G. & Kadler, K.E. Procollagen trafficking, processing and fibrillogenesis. *J Cell Sci* **118**, 1341-1353 (2005).
100. Rhudy, R.W. & McPherson, J.M. Influence of the extracellular matrix on the proliferative response of human skin fibroblasts to serum and purified platelet-derived growth factor. *J Cell Physiol* **137**, 185-191 (1988).
101. Selman, M., *et al.* Gene Expression Profiles Distinguish Idiopathic Pulmonary Fibrosis from Hypersensitivity Pneumonitis. *Am J Respir Crit Care Med* (2005).
102. Selman, M., Pardo, A. & Kaminski, N. Idiopathic pulmonary fibrosis: aberrant recapitulation of developmental programs? *PLoS Med* **5**, e62 (2008).
103. Muro, A.F., *et al.* An essential role for fibronectin extra type III domain A in pulmonary fibrosis. *Am J Respir Crit Care Med* **177**, 638-645 (2008).
104. Strutz, F., *et al.* Identification and characterization of a fibroblast marker: FSP1. *J Cell Biol* **130**, 393-405 (1995).
105. Ask, K., *et al.* Progressive pulmonary fibrosis is mediated by TGF-beta isoform 1 but not TGF-beta3. *The international journal of biochemistry & cell biology* **40**, 484-495 (2008).
106. Endo, M., *et al.* Induction of arginase I and II in bleomycin-induced fibrosis of mouse lung. *Am J Physiol Lung Cell Mol Physiol* **285**, L313-321 (2003).
107. Sato, M. Upregulation of the Wnt/beta-catenin pathway induced by transforming growth factor-beta in hypertrophic scars and keloids. *Acta dermato-venereologica* **86**, 300-307 (2006).
108. Zuo, F., *et al.* Gene expression analysis reveals matrilysin as a key regulator of pulmonary fibrosis in mice and humans. *Proc Natl Acad Sci U S A* **99**, 6292-6297 (2002).

-
109. Leask, A. & Abraham, D.J. The role of connective tissue growth factor, a multifunctional matricellular protein, in fibroblast biology. *Biochemistry and cell biology = Biochimie et biologie cellulaire* **81**, 355-363 (2003).

[I] <http://www.stanford.edu/~rnusse/WNTwindow.html>

[II] <http://www.biocolor.co.uk/sircol.html>

8. Erklärung

Ich erkläre: Ich habe die vorgelegte Dissertation selbständig, ohne unerlaubte fremde Hilfe und nur mit den Hilfen angefertigt, die ich in der Dissertation angegeben habe. Alle Textstellen, die wörtlich oder sinngemäß aus veröffentlichten oder nicht veröffentlichten Schriften entnommen sind, und alle Angaben, die auf mündlichen Auskünften beruhen, sind als solche kenntlich gemacht. Bei den von mir durchgeführten und in der Dissertation erwähnten Untersuchungen habe ich die Grundsätze guter wissenschaftlicher Praxis, wie sie in der "Satzung der Justus-Liebig-Universität Gießen zur Sicherung guter wissenschaftlicher Praxis" niedergelegt sind, eingehalten.

9. Danksagungen

Ich danke Prof. Dr. med. Werner Seeger für das Schaffen eines Umfeldes, welches Medizinstudenten ermöglicht, im Rahmen ihrer Promotion medizinische Grundlagenforschung kennenzulernen.

Bei Prof. Dr. Oliver Eickelberg bedanke ich mich für die Überlassung des Themas und die Möglichkeit, in seinem Labor Einblicke in wissenschaftliches Denken, Arbeiten und Präsentieren zu bekommen. Mit seinem Wissen und seinem Optimismus hat er mich immer wieder ermutigt, herausgefordert und motiviert.

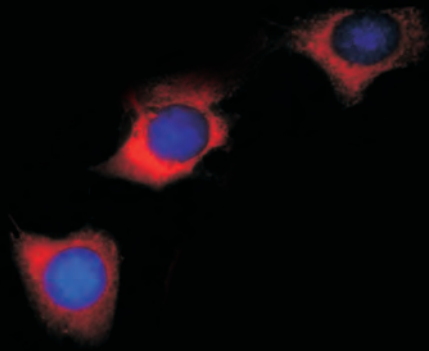
Ganz besonders danke ich Dr. Dr. Melanie Königshoff für die ausgezeichnete Betreuung und ihr persönliches Engagement auf theoretischer, praktischer und menschlicher Ebene über die gesamte Zeit, sowohl aus der Nähe als auch aus der Ferne in den letzten Monaten.

Bei Simone Becker und Andreas Jahn bedanke ich mich herzlich für ihre Tipps und Ratschläge beim Erlernen der Methoden und die Hilfsbereitschaft beim Zurechtfinden im Labor .

Ein besonderer Dank gilt Nisha Balsara und Eva-Maria Pfaff für freundschaftliche Zusammenarbeit und ein immer offenes Ohr.

Dem gesamten ehemaligen „Eickelberg lab“ danke ich für eine sehr schöne und lehrreiche Zeit.

Abschließend danke ich meiner Familie und Christian für Geduld, Unterstützung und stetigen Rückhalt.



édition scientifique

VVB LAUFERSWEILER VERLAG

VVB LAUFERSWEILER VERLAG
STAUFBENGRING 15
D-35396 GIESSEN

Tel: 0641-5599888 Fax: -5599890
redaktion@doktorverlag.de
www.doktorverlag.de

ISBN: 978-3-8359-5627-8



9 783835 956278